REGULATION OF THE PORE-FORMING TRANSLOCON OF THE TYPE III SECRETION SYSTEM BY THE EspC SERINE PROTEASE IN ENTEOPATHOGENIC *ESCHERICHIA COLI*

by

Leticia Tavares Gomes

June 2016

CATÓLICA

UNIVERSIDADE CATÓLICA PORTUGUESA | PORTO

Escola Superior de Biotecnologia

REGULATION OF THE PORE-FORMING TRANSLOCON OF THE TYPE III SECRETION SYSTEM BY THE EspC SERINE PROTEASE IN ENTEROPATHOGENIC *ESCHERICHIA COLI*

Thesis presented to *Escola Superior de Biotecnologia* of the *Universidade Católica Portuguesa* to fulfill the requirements of Master of Science degree in Microbiology

by

Leticia Tavares Gomes

Place: Centre of Interdisciplinary Research in Biology – Collège de France, Paris

Supervision: Guy TRAN VAN NHIEU

June 2016

Aos meus pais,

por tudo o que fizeram e construiram,

por continuarem a fazer tudo pelos filhos.

Resumo

As bactérias do grupo *Escherichia coli* enteropatogénica (EPEC) são uma das maiores causas de diarreia fatal em crianças com menos de cinco ano nos países em desenvolvimento. A virulência de EPEC depende da presença do sistema de secreção do tipo III (SST3). O SST3 é constituído por um corpo basal situado entre a membrana externa e interna da bactéria, prolongado por uma agulha que é projetada a partir da superfície da bactéria. No caso de EPEC, a agulha do SST3 é prolongada por um filamento formado pela proteína hidrofílica, EspA. Depois de contactar com a célula hospedeira, o sistema ativa a secreção de duas proteínas hidrofóbicas, EspD e EspB. Estas proteínas inserem-se na membrana plasmática da célula hospedeira para formar o transclocão. O translocão é uma estrutura chave para formar o poro na membrana da célula hospedeira pelo qual os efetores são inseridos na célula.

O laboratório onde se realizou este trabalho estuda o papel da proteína EspC, que pertence à família SPATE (*serine protease autotransporter of Enterobacteriaceae*), na regulação e funcionamento do translocão. EspC é secretada pelo sistema de secreção do tipo V, sendo independente do SST3. Foi demonstrado que EspC tem um papel importante no controlo da formação do poro membranar e da virulência mediada pelo SST3. EspC tem preferencialmente como alvo os complexos de EspA-EspD, envolvidos na formação do poro membranar, presumivelmente após o destacamento do translocão do filamento da agulha.

Este trabalho de estágio utilizou procedimentos de purificação para isolar o complexo EspA-EspD sensível à proteólise de EspC com o objetivo de realizar a caracterização estrutural deste complexo por Microscopia Eletrónica. Implementamos várias fases de purificação distintas para aumentar a pureza das amostras contendo os complexos desejados. Conseguimos isolar complexos homogéneos contendo EspA que mostram um estrutura em forma de anel com um diâmetro externo de 10 nm e um interno de 4 nm.

Abstract

Enteropathogenic *E. coli* (EPEC) is a major cause of fatal diarrhea in childs under 5 years in developing countries. EPEC virulence is dependent on the presence of type III secretion system (T3SS). T3SSs are used by many pathogenic Gram-negative bacteria to inject bacterial effectors into host cells. T3SSs consist of a basal body embedded in the bacterial outer and inner membrane, prolonged by a needle protruding from the bacterial surface. In the case of EPEC, the T3SS needle is extended by a filament formed by hydrophilic EspA protomers. Upon cell contact, the system triggers the secretion of two hydrophobic proteins EspD and EspB, that insert in the host cell plasma membrane to form the translocon. The translocon is critical for the injection of type 3 effectors, presumably by forming a pore into host cell plasma membranes through which the effectors are channeled.

The host lab studies the role of EspC, a serine protease autotransporter of Enterobacteriaceae (SPATE) family, on the regulation of the translocon function. EspC is a protein secreted by EPEC by a type V secretion system independently of the T3SS, although the translocation into epithelial cells requires active type III secretion. EspC has been shown to play a role in controlling pore formation and cytotoxicity mediated by the T3SS. EspC was shown to preferentially target an EspA-EspD complex, involved in the T3SS-dependent pore formation, supposedly following detachment of the translocon from the T3SS needle filament.

This internship work took advantage of fractionation procedures worked out to isolate the EspA-EspD complex sensitive to EspC proteolysis, with the aim to perform a structural characterization of this complex by electron microscopy analysis. In this study, we increased the yield of EspA-EspD complex purification, that for the first time allowed the detection of EspB together with EspA-EspD complexes. We implemented additional purification steps to increase the purity of protein complexes. We were able to isolate homogenous EspA-containing complexes showing a ring-link structure with an external diameter of 10 nm of and a 4 nm-inner diameter.

ACKNOWLEDGMENTS

I would like to thank all the persons that make this experience unforgettable. Paris is always a good idea.

First, I would like to thanks Guy Tran Van Nhieu, for the opportunity to work at Collège de France, in his team, and for all the knowledge that he passed to me. Thank you for all the time that you spend correcting this master thesis.

Thanks to all the team: César, for all the help in the lab, all the discussions and fun that we had together; Mariette for the support in all situations, thank you for be the one that always know what to say and how to help; Javier, thank you for all your tips and tricks in the lab, for all the availability to help; Stephane, Daniel and Nicole, thank you for all the help and the good time that we spend together!

All the good friends that I've made at Collège. A special thanks to Richard that since the beginning was here to hear all the fears and expectations that I had. Marion and Stephanie, you already know… our triplet is the best.

A special word to the ones that walked by my side in Coimbra – "Saudade desta cidade, levo comigo P'rá vida". Obrigada à Universidade de Coimbra, à Associação Académica de Coimbra e às pessoas que por lá passaram comigo.

Obrigada a quem sempre me incentivou a correr atrás dos meus objetivos, ainda que algumas decisões não tenham sido fáceis. Obrigada às de sempre, por tudo que somos juntas.

Obrigada ao Porto que me acolheu. À Escola Superior de Biotecnologia, especialmente aos professores com que me cruzei, alguns dos melhores da minha vida de estudante. Aos colegas, especial à Dandára por ter sido a minha metade em todos os trabalhos, no dia a dia do Porto e no skype.

Obrigada às minhas tias e madrinha, pelo suporte que foram para mim em Paris. Especialmente à tia São, que me acolheu com tudo o que tinha.

À Barbara e ao Nelson, por me terem acompanhado sempre!

Aos meus pais. Faltam-me as palavras para agradecer tudo aquilo que me permitiram viver. Obrigada por me terem deixado caminhar sozinha, por me terem visto cair, mas por estarem lá para me levantarem. Desculpem pelos momentos menos bons… Mas a força que sempre me guiou, foi o nunca vos querer desiludir. Sei que vêm esta minha vitória como vossa, e ela é toda dedicada a vocês. São o melhor de mim, a minha inspiração de vida!

CONTENTS

ABBREVIATIONS

E. coli – Escherichia coli

EPEC – Enteropathogenic Escherichia coli

SST3 – Sitema de Secreção Tipo III

T3SS – Type III Secretion System

SPATE – Serine Protease Autotransporters of Enterobacteriaceae

AE – Attachment and Effacing

IECs – Intestinal Epithelial Cells

LEE – Locus of enterocyte effacement

Tir – Translocated Intimin Receptor

BFP – Bundle-forming pili

Ler – LEE-encoded regulator

H-NS – Histone-like nucleoid-structuring protein

Hfq – RNA binding protein

T3SA – Type III Secretion Apparatus

LPS – Lipopolysaccharide

EspA – Hydrophilic protein

EspD – Major hydrophobic protein

EspB – Minor hydrophobic protein

EM – Electron Microscopy

NC – Needle Complex

TC – Tip Complex

RBC – Red blood Cell

NMR – Nuclear Magnetic Resonance

DOC – Sodium deoxycholate

FAK – Focal adhesion kinase

TCA – Trichloroacetic acid

ON – Overnight

FPLC – Flow Pressure Liquid Chromatography

L – Load

FT – Flow Through

SEC – Size Exclusion Chromatography

INTRODUCTION

I. *Escherichia coli*

Theodor Eschrich was the first to report the isolation of a microorganism from infant stool which he named *Bacterium coli commune* in 1885 (reprinted in English: Eschrich and Bettelheim, 1988). Only in 1954, the name *Escherichia coli* was fully adopted (Cowan, 1954). In early studies, it was considered as a harmless commensal of the gastrointestinal tract in warm-blooded animals. Because some strains were found not to invade cells or release diffusible toxins, doubts about their pathogenic potential were raised in the 1960s and 1970s. The isolation of pathogenic bacteria inducing diarrhea in human volunteers provided the decisive evidence for *E. coli* strains as true human pathogens (Levine *et al*., 1978).

The diseases caused by pathogenic *E. coli* strains affect the gastrointestinal tract, as well as extraintestinal sites such as the urinary tract, the bloodstream, and central nervous system (Croxen and Finlay, 2010). Pathogenic *E. coli* strains have been classified in two main groups: diarrhoeagenic *E. coli* or extraintestinal *E. coli*. Enteropathogenic *E. coli* (EPEC), enterohaemorrhagic *E. coli* (EHEC), enterotoxigenic *E. coli* (ETEC), enteroinvasive *E. coli* (EIEC), enteroaggregative *E. coli* (EAEC) and diffusely adherent *E. coli* (DAEC) correspond to the six well studied pathovars that are diarrhoeagenic. The extraintestinal group contains two pathovars: the uropathogenic *E. coli* (UPEC) and neonatal meningitis *E. coli* (NMEC).

The genome size of *E. coli* strains can differ by a million base pairs between commensal and pathogenic variants – comparative genomics studies between 186 *E. coli* genomes have shown a "core genome" of about 1,700 homolog gene clusters, and a flexible gene pool of about 16,400 gene clusters (Kaas *et al*., 2012). The pathogenicity of *E. coli* is regulated by the flexible gene pool trough the gain or loss of genetic material (Croxen *et al*., 2013). Horizontal gene transfer is an important way to disseminate traits in recipient organisms and is crucial to promote the fitness and survival of the pathogen during infection. Pathogenicity islands (PAIs) are clusters of virulence genes found on plasmids or integrated into the chromosome, that are usually bordered by mobile genetic elements, PAIs are not found in non-pathogenic bacteria.

II. Enteropathogenic *E. coli*

EPEC was the first diarrheagenic *E. coli* to be identified, being responsible for a series of outbreaks of infantile diarrhea in the 1940s and 1950s. E2348/69 strain has been used worldwide as a prototype strain to study EPEC and the complete sequence of the strain was published in 2009 (Igushi *et al*., 2009). EPEC is a non-invasive microorganism that does not produce enterotoxins. It was with studies on the E2348/69 strain that the firsts insights in the pathogenic strategy of EPEC began to emerge. With the discovery of LEE (Locus of Enterocyte Effacement), EPEC was classified in a group of bacteria known as attaching and effacing (A/E) pathogens. AE pathogens classification is based on their ability to form distinctive lesions on the surfaces of intestinal epithelial cells (IECs). The EPEC group is subdivided in atypical and typical EPEC based on the presence or absence of the *E. coli* adherence factor plasmid, respectively (pEAF) (Kaper *et al*., 2004). While humans are the only known reservoir for typical EPEC, atypical strains have been isolated from human and animal sources like dogs, rabbits, monkeys and sheep (Moura *et al*., 2009).

The enteropathogenic *E. coli* is a major cause of fatal diarrhea in childs under 5 years in developing countries. The prevalence of EPEC infection varies from the studies and the data showed until today, depend on the population of study, and age distribution or the methods used for detection or diagnosis. Also, the geographic region or the socioeconomic class may influence the epidemiology of EPEC. Based on molecular methods and identification of intimin gene, for example, EPEC was found responsible for 5 to 10% of pediatric diarrheal episodes in developing countries, while if the determination is made based on the HEp-2 adherence pattern or serotyping, the estimated prevalence is higher, going from 10 to 20% (Ochoa *et al*., 2008).

EPEC causes diarrhea often accompanied with fever, vomiting and dehydration in children under 5 years. EPEC infections often lead to acute diarrhea, but persistent cases have also been reported to last more than 2 weeks (Nataro and Kaper, 1998). In comparison to infection with other diarrheal pathogens such as adenovirus, rotavirus, *Campylobacter* and *Salmonella*, infection with EPEC is more likely to lead to development of persistent diarrhea and hospitalization (Nguyen *et al*., 2006).

III. EPEC Pathogenesis

AE lesions are a hallmark of EPEC pathogenesis, characterized by effacement of brush border microvilli at the site of bacterial attachment. The disruption of the intestinal brush border is accompanied by the formation of actin pedestals that extend from the surface of the epithelium into the lumen. The pedestal-like structures are produced following secretion of a bacterial receptor protein (Tir) through the Type III secretion System (T3SS). The T3SS is absolutely required for EPEC pathogenesis.

A three-stage model of EPEC pathogenesis was first described by Donnenberg and Kaper, including localized adherence to host cells, signal transduction and intimate attachment (Donnenberg and Kaper, 1992). During intimate attachment, a series of bacterial effectors proteins are injected into host cells, where they interfere with actin dynamics and others host cellular processes (Dean and Kenny, 2009). The three-stage model is represented in Figure 1.

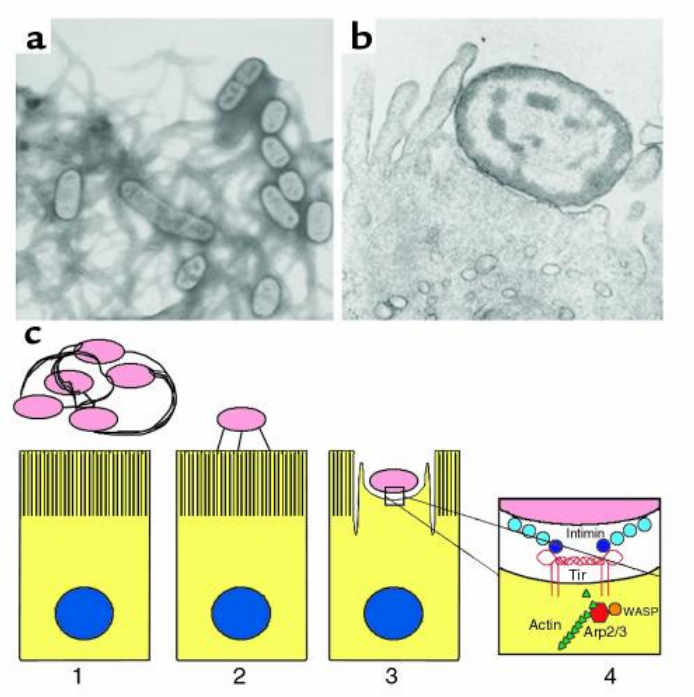

Figure 1. Attaching and Effacing lesions induced by EPEC. (**a**) Electron micrograph of EPEC expressing type IV fimbria known as bundle-forming pili (BFP); (**b**) Electron micrograph of an EPEC bacterium engaged in attaching and effacing activity with a host intestinal epithelial cell. Note the loss of microvilli and the formation of a cuplike pedestal to which the bacterium is intimately attached; (**c**) A model of EPEC pathogenesis. (Donnenberg *et al*., 2001).

A bacterial aggregate, connected by bundles of BFP fibers, is shown near an intestinal epithelial cell (Fig. 1a). As infection proceeds, the bacteria detach from the pilus fibers, disaggregate, and attach to the host cell through a surface appendage that contains EspA (Fig. 1b). It is believed that Tir, EspB, EspD and EspF (see table 1.) travel through this appendage to the host cell. EspF is not required for attaching and effacing activity but plays a role in disruption of intestinal barrier function and host cell death. EspB, EspD and Tir are required for attaching and effacing activity (Fig. 1c).

Table 1. Summary of virulence factors in EPEC O127:H6 adapted from K.J. Spears *et al.* 2006

Virulence factor	Encoding region	Function
Adhesins		
Type 1 fimbriae	*fim* operon	Adherence to α-D-mannose-containing glycoproteins
Type IV pilus (Bfp)	14 genes in the EAF plasmid	Initial adherence specificity to phosphatidylethanolamine
OmpA	*ompA*	Mediates HeLa cell adherence
Escherichia coli factor for adherence (Efa)	(O157) *lifA*	Regulation of T3SS
Flagellin	*fliC*	Motility abd adherence
LEE-encoded		
Intimin	*eae* (LEE5)	Intimate attachment adhesion molecule
Translocated intimin	*tir* (LEE5)	Intimate attachment; AE lesion formation; actin polymerization
Receptor (Tir)		
Mitochondrion-associated protein (Map)	*map* (LEE5)	Disruption of TER; mitochondrial membrane potential; filopodium formation
EspF	*espF* (LEE4)	Disruption of TER; mitochondrial membrane potential; cell death
EspH	*espH* (LEE3)	Disruption of cytoskeleton
Non-LEE-encoded		
Secreted serine protease	*espC*	Epithelial/tight junction disruption, mucinase, interference with complement cascade

A. Adherence

The localized adherence phenotype of EPEC is the result of a surface appendage known as the bundle-forming pilus (BFP), which is encoded by the EAF plasmid. BFP is responsible for the formation of bacterial clusters, because of its ability to form reversible aggregates into rope-like bundles. If any of the genes required for the formation of BFP is inactivated by mutation, the bacteria fails to form aggregates and is not able to display localized adhesion (Donnenberg *et al.,* 2000).

A/E lesions are caused by the ability of bacteria to intimately attach to the host cell membrane, destroying the microvilli and inducing the formation of pedestal-like structures enriched in cytoskeletal proteins (Fig. 1b). The LEE is a 35 kb genetic locus responsible for this event. It has been shown that the LEE from EPEC strain E2348/69 cloned into a non-pathogenic *E. coli* strain is sufficient to confer attaching and effacing activity (Frankel *et al*., 1998).

B. Signal transduction and intimate attachment

Formation of the A/E lesions occurs by subversion of actin dynamics within host cell by EPEC through the injection of type III effectors. It is mediated by the interaction between intimin, a bacterial surface protein and the bacterial translocated intimin receptor, Tir. All the strains capable to induce the A/E lesions have the *eae* gene, which encodes intimin.

IV. Locus of enterocyte effacement (LEE)

The genes encoding T3SS components and related proteins including regulators, chaperones, and some effectors, are clustered in a 35-kb chromosomal region termed the locus of enterocyte effacement (LEE). The LEE contains 41 genes organized in five major operons, designated *LEE1*, *LEE2*, *LEE3*, *LEE4* and *LEE5*, and several smaller transcriptional units (Mellies *et al*. 2007). The *LEE1*, *LEE2*, and *LEE3* operons encode the type III apparatus including a basal body that spans the inner and outer membranes, prolonged by a needle composed of EscF. The *LEE4* operon encodes the EspA protein that polymerizes to form the filament that prolongs the T3SS needle; EspB and EspD form the translocon in the host cell membrane; EspF is injected into the host cell and targeted to the mitochondria, where it plays a role in the cell death pathway. The *LEE5* operon encodes the Tir and intimin proteins, which are necessary for intimate attachment to the host epithelium; and CesT, a chaperone for Tir (Mellies *et al*. 2007).

A. LEE regulation

The regulation of virulence genes expression in EPEC in not completely understood. The *LEE1*-located Ler (LEE-encoded regulator) plays a central role in the regulation of the AE phenotype.

The expression of *LEE* genes is thermo-regulated: AE lesions do not form if the bacteria are incubated at 28°C prior to infecting host cells at 37°C. H-NS (histone-like nucleoid-structuring) is responsible for repressing *LEE1* at 27°C by binding to *LEE1*, *LEE2* and *LEE3*. At 37°C H-NS are not able to bind to these loci, therefore protein secretion via T3SS in EPEC occurs maximally at 37°C (Mellies *et al*., 2007). Under inducible conditions, H-NS mediated repression of *LEE1* is relieved and the transcription of *ler* is induced (Bhatt *et al*., 2011). Ler primarily activates transcription from the other LEE operons that allows the synthesis and assembly of the T3SS. Ler is 15kDa protein with a strong control over the LEE genes. It has been shown that a *ler* mutant of the prototypical EPEC strain E2348/69 severely decreased its ability to form AE lesions in epithelial cells in culture (Elliott *et al*., 2000).

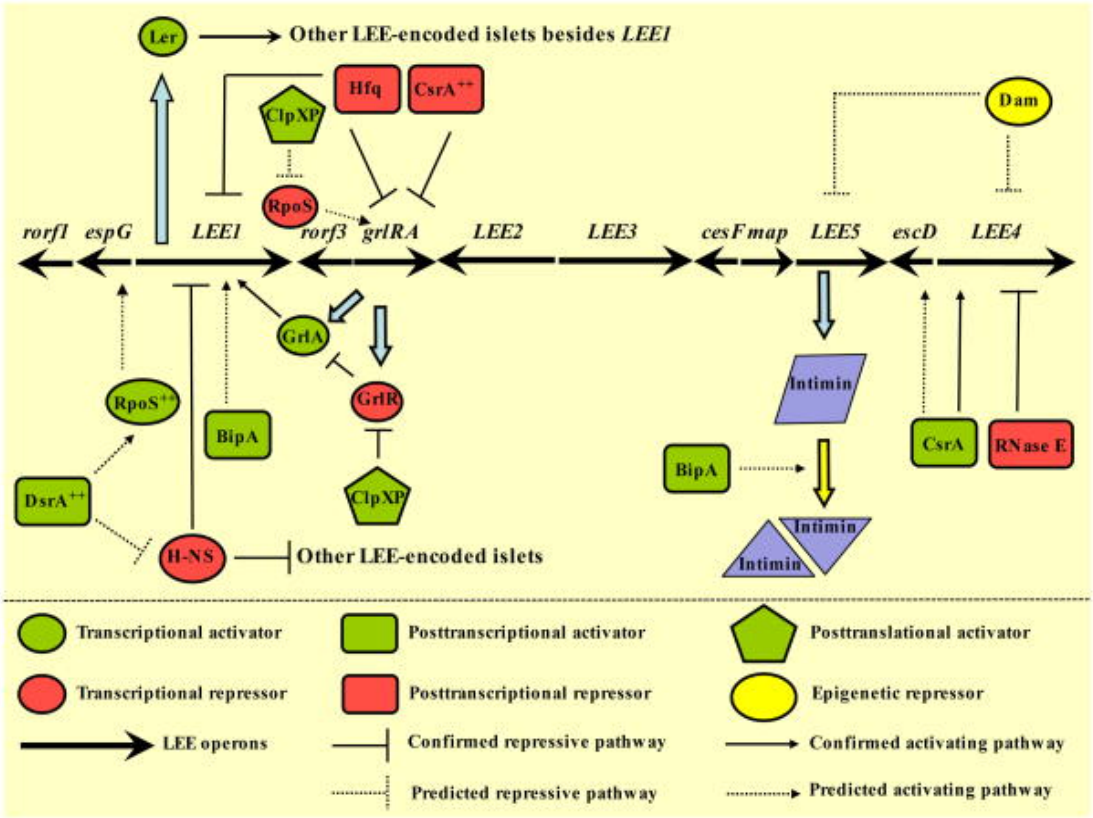

Figure 2. Transcriptional and extratranscriptional control of LEE. (From Bhatt *et al*., 2011)

When reaching host body temperature, Ler increases the transcription of the *LEE2*, *LEE3*, *LEE4* and *LEE5* operons. Among others, Ler also increases the expression of EspC protein. EspC will further discussed in the chapter VIII (EspC serine protease). During infection of cultured cells, Ler-induced expression is necessary only during the early stages of the EPEC infection process (Leverton *et al*., 2005). By real-time PCR the Leverton demonstrated that transcription of the EPEC *LEE3*, *LEE4* and *LEE5* operons increased over 3 hours post-

infection, while the expression of *LEE1*, carrying *ler*, decreased during the same period in a Ler-dependent manner (Leverton *et al*., 2005). This shows that during infection, other factors regulate Ler function leading to repression of LEE1. Mutation of *ler* in EPEC also affects the pattern of EPEC adherence (Elliott *et al*., 2000). Wild-type EPEC normally shows localized adherence to cells, with the formation of microcolonies. Mutation of *ler* in EPEC is rather associated with the appearance of a diffuse adherence phenotype. Interestingly, electron microscopy studies have shown that *ler* mutants present changes in fimbrial expression accompanied by the alterations in adherence.

Moreover, Ler is also regulated by post-translational factors, such as Hfq. Hfq is a conserved RNA-binding protein that regulates diverse cellular processes through post-transcriptional control of gene expression, functioning as a chaperone of sRNAs. Hfq has been shown to have a critical impact on bacterial pathogenicity in a wide array of bacterial species (Shakhnovich *et al*., 2009). It is known that in EHEC *hfq* mutants increase Ler production leading to an increase in the quantities of T3SS effectors into the supernatant even though an *hfq* mutant shows compromised growth.

The ability to form AE lesions, intimate attachment to the host cell and formation of "pedestals"-like structures are characteristics shared with Enterohaemorrhagic *Escherichia coli* (EHEC) that also expresses a T3SS and shows genetic similarities with EPEC. (Mellies *et al*., 2007). The T3SS is used by Gram-negative bacteria to translocate effector proteins into the cytosol of eukaryotic host cells while, in the case of EPEC, remaining extracellular (Frankel *et al*., 1998).

V. Type III Secretion System (T3SS)

Michiels *et al*. observed that the *Yersinia* "Yop" proteins were translocated into host cells without the Sec-dependent cleavage of their N-terminal sequence, leading to the discovery of a new secretion system, named Type III Secretion System (Michiels *et al*., 1991).

The Type III Secretion System (T3SS) is involved in a wide spectrum of interactions, from mutualism to pathogenesis, between Gram-negative bacteria and various eukaryotes, including plants, fungi, protozoa and mammals (Egan *et al.*, 2014). T3SSs are highly homologous to flagella, which drive cell motility, but are specialized in the delivery of bacterial effectors in to eukaryotic cells (Abby and Rocha, 2012).

Bacteria may express one or several T3SSs dedicated to the injection of specific subsets of effectors and show different infectious strategies. For example, *Salmonella* expresses two T3SSs, one to translocate proteins required for cell invasion during the early stage of infection and a second for proteins that are needed for intracellular survival and replication inside the phagosome (Shea *et al*., 1996). *Shigella*, on the other hand, only expresses one T3SS to invade intestinal epithelial cells and to replicate freely in the cytosol of the infected cells (Clerc *et al*., 1986).

Because they play a critical role in the virulence of human and plant pathogens (*E. coli*, *Shigella*, *Salmonella*, *Yersinia*, *Vibrio*, *Pseudomonas*, *Chlamydia*), T3SSs represent an attractive target for the discovery or design of novel anti-infective agents and vaccine approaches.

A. General Structure

T3SSs are highly complex nanomachines consisting of the type III secretion apparatus (T3SA) and type III effectors and chaperones. T3SA contain between 20 to 30 components, with at least 9 of them conserved among plants- and animal-pathogenic bacteria (Bogdanove *et al*., 1996). Despite the high degree of homology of some T3SA components, the field is in need of a general nomenclature, such as the one used for flagellar components from different species to facilitate the cross-species comparisons. Table 2 adapted from Notti *et al*., 2016, illustrate the diversity of names of used for T3SA orthologs and a recently proposed nomenclature.

Table 2. Unified nomenclature for the homologous core components of the T3SS, adapted from Notti RQ, 2016

	Universal Nomenclature	Salmonella	*Shigella*	EPEC	*Yersinia spp.*	*Pseudomonas aeruginosa*
Basal Body	SctC	InvG	MxiD	EscC	YscC	PscC
	SctD	PrgH	MxiG	EscD	YscD	PscD
	SctJ	PrgK	MxiJ	EscJ	YscJ	PscJ
Inner Rod	SctI	PrgJ	MxiI	EscI	YscI	PscI
Needle Filament	SctF	PrgI	MxiH	EscF	YscF	PscF
Needle Length Regulator	SctP	InvJ	Spa32	EscP	YscP	PscP
Inner Membrane Machinery	SctV	InvA	MxiA	EscV	LcrD	PcrD
	SctR	SpaP	Spa24	EscR	YscR	PscR
	SctS	SpaQ	Spa9	EscS	YscS	PscS
	SctT	SpaR	Spa29	EscT	YscT	PscT
	SctU	SpaS	Spa40	EscU	YscU	PscU
Needle Tip and Translocon		SipB	IpaB	EspD	YopB	PopB
		SipC	IpaC	EspB	YopD	PopD
		SipD	IpaD	EspA	LcrV	PcrV
Coiled Coil Linker	SctO	InvI	Spa13	EscA	YscO	PscO
ATPase	SctN	InvC	Spa47	EscN	YscN	PscN
Sorting Platform	SctQ	SpaO	Spa33	SepQ	YscQ	PscQ
	SctK	OrgA	MxiK		YscK	
	SctL	OrgB	MxiN	EscL	YscL	PscL
Export Regulator	SctW	InvE	MxiC	SepL/SepD	YopN	PopN

The function of this nanostructure is to deliver bacterial effectors into the cytosol of eukaryotic target cells. While there may be minor differences between species, T3SAs share a general structure and functional properties.

T3SAs consist of a basal body spanning the two bacterial membranes and the peptidoglycan, prolonged by a hollow needle protruding from the bacterial surface. In some instances, the T3SA needle may be connected to a filament (animal pathogens) or to a long pilus (plant pathogens) (Cornelis, 2010). The length of the needle is tightly regulated (Cornelis, 2006), presumably to allow the precise exposure of the so-called "tip complex" at the bacterial LPS surface layer (Mota *et al.*, 2005). The tip complex is composed of two proteins, one hydrophobic and one hydrophilic. The tip complex is involved in the negative regulation of the T3SS and plays an important role in the recognition of the host cell. It is proposed to act as a scaffold for the assembly of the minor hydrophobic protein. The minor

hydrophobic protein is secreted upon cell contact and together with the major hydrophobic protein, is required to allow translocation of proteins from the bacterium to the host cell cytoplasm. Because the hydrophilic- as well as translocon proteins are required for type III effector injection into host cells, these are also called "translocator" components.

In the past years the application of structural and biochemical approaches to the study of the T3SS has provided numerous insights into the assembly and function of the system. We will present a general overview of T3SSs based on the *Salmonella*, *Yersinia* and *Shigella* systems that are the best characterized.

B. Biogenesis of the T3SS

The first studies on the biogenesis of T3SA have been performed in Salmonella (Diepold and Wagner, 2014). Today it is accepted that the injectisome assembly starts with the Sec-dependent formation of a stable ring in the outer membrane, the secretin composed of SctC, followed by the formation of a set of rings associated with the inner membrane, the MS ring composed of SctD and SctJ (Figure 3, panel 1-6). One of the studies that support this proposal shows that the secretin and MS rings associate in a process independent of type 3 secretion, since it can occur in the absence of the T3SS ATPase (Kubori *et al*., 2000). In support for an initial role in T3SA assembly Schraidt *et al.* showed that in the absence of secretin fewer complexes were observed, indicating a role for the secretin in the complex stability (Schraidt *et al.,* 2010). In accordance with those findings, in the case of EPEC it was found that all three basal proteins (EscCDJ) were required for assembly of the T3SA (Ogino *et al.,* 2006).

Assembly of the inner and the outer membrane rings (Figure 3, panel 7) is presumed to allow the recruitment of the cytoplasmic components (Figure 3, panel 8 and 9). The cytosolic components (Figure 3, panel 8) assemble at the proximal side of the MS rings, as observed for the flagellum (Diepold *et al.*, 2010). The type III ATPase and the C ring require the presence of each other for their recruitment. Both of them interact with accessory proteins (YscK and YscL in the case of *Yersinia*) to assemble at the proximal side of the basal body (Diepold *et al.*, 2012). The observation that the C ring, stalk and accessory proteins co-purify with the cytosolic domain of the switch protein SctU suggests that the switch protein provides the docking site (Botteaux *et al.*, 2010).

The next step of the T3SS assembly is the formation of the needle filament (Figure 3, panel 10). The assembly of SctUVJ with SctC and SctD allows the recruitment of the cytoplasmic components, leading to a functional T3SS. At this step the T3SS secretes the

early substrates, among others the needle filament protein that needs the co-secretion of the inner rod and the needle length regulator (Chapter V, D).

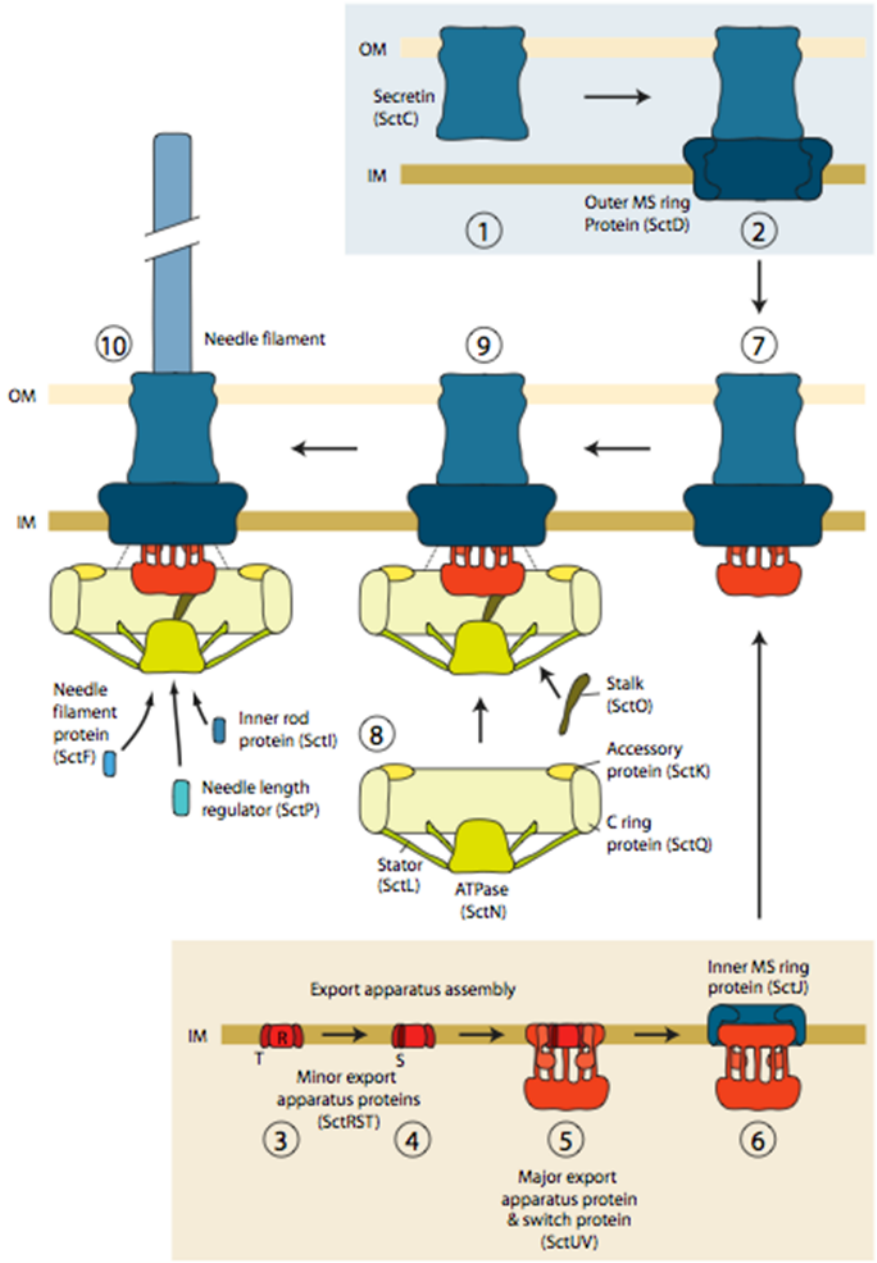

Figure 3. Model of injectisome assembly. The secretin ring in the OM assembles independently and triggers the assembly of the outer MS ring (1, 2). In the inner membrane, MS ring assembly nucleates the minor export apparatus proteins and progresses via the recruitment of the switch protein and major export apparatus protein (3–5). Both the secretin – outer MS ring protein complex and the export apparatus complex can associate with the inner MS ring protein (6, 7). Integration of the two assemblies into one complex allows subsequent recruitment of the cytoplasmic components (7–9). This leads to a functional type III secretion system, firstly secreting early substrates, amongst others the components of the inner rod and needle filament proteins (10). From Diepold and Wagner 2014.

The secretion of the needle subunit is assisted by a chaperone, which prevents premature filament formation in the bacterial cytosol (Sal-Man *et al.*, 2013). This leads to needle elongation that occurs by subunit polymerization at the distal end, through partial refolding of the subunit protomers from alpha-helix into beta-strand conformation (Poyraz *et al.,* 2010). The length of the needle is controlled by a mechanism involving the "molecular ruler" protein SctP and the switch protein SctU.

Several studies have demonstrated that effector protein translocation starts within seconds after host cell contact and that the translocation rates of effector proteins can vary between effectors (Enninga, 2005; Rosenshine, 2009). The different rates suggest that a hierarchy of effectors' translocation is required for the efficient manipulation of host cellular pathways. Furthermore, the temporal regulation of effector protein translocation might prevent interference of effector proteins with antagonistic activities, as shown for SopE, that induces actin polymerization, and SptP that disrupts the actin cytoskeleton in the case of *Salmonella spp*.

C. The basal body and Needle Complex

The basal body is composed of the secretin in the outer membrane connected by a hinge region to the MS rings associated with the inner membrane (Schraidt *et al.*, 2011). EM reconstructions of the *Salmonella Typhimurium* injectisome have shown that the basal body is formed by InvG, PrgH and PrgK (SctC, SctD and SctJ in the universal nomenclature) (Marlovits *et al*., 2004). In Salmonella, quantitative amino acid analysis revealed that the components of the base InvG:PrgH:PrgK are present in 1:1:1 molar ratio, suggesting that the three proteins are structurally linked by a shared rotational symmetry. The symmetry of inner membrane MS rings' structure appears to be conserved among T3SSs (e.g.: *Shigella*, Hodgkinson *et al*., 2009), while the stoichiometry of the secretin, InvG (SctC) may vary between species (e.g.: *Yersinia*, Kudryashev *et al*., 2013).

Within the lumen of the basal body, SctI forms a cylindrical “inner rod” structure that supports the extracellular needle formed of SctF. The needle complex protruding from the extracellular side of the T3SS basal body is formed by a helical assembly of SctF, with an outer diameter of 8 nm and an inner diameter of 2 - 3 nm (Radics *et al*., 2013). In the case of EPEC, a filament formed of polymerized EspA prolongates the needle structure composed of EscF (SctF). This filamentous extension of the hydrophilic protein from the needle is unique

to EPEC family (Knutton *et al*., 1998). The EspA filament has an internal diameter of 2.5 nm, similar to that of the EscF needle (Cheung *et al*., 2015). This suggests that the function of the EspA filament is to extend the T3SS transport conduit to reach the target cell membrane through the intestinal glycocalyx (Mueller *et al.*, 2008).

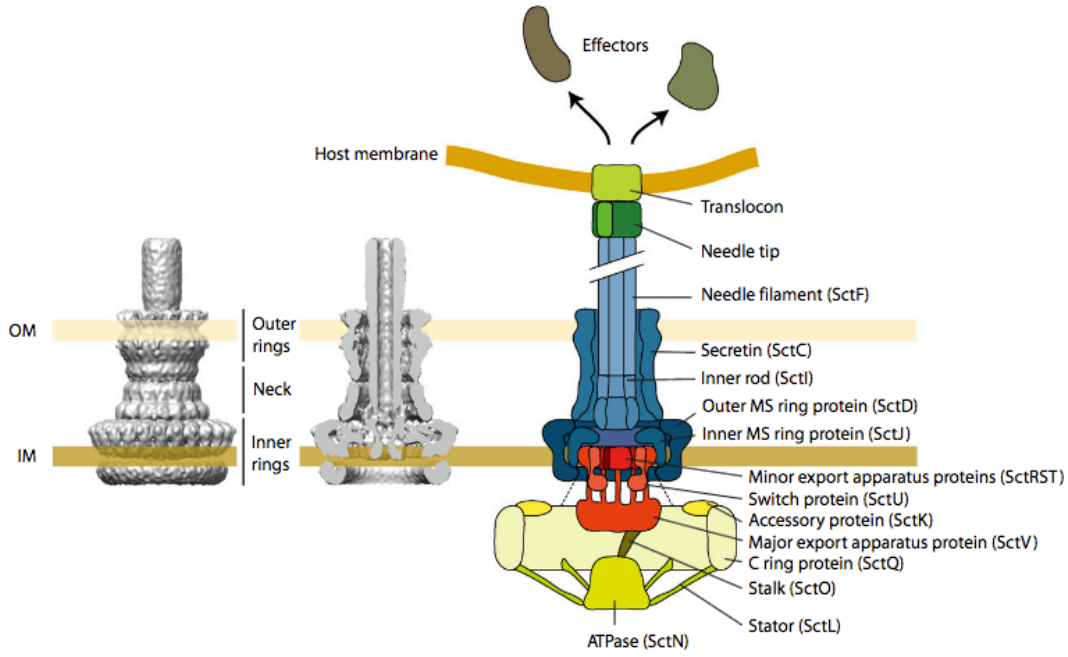

Figure 4. Overview of the injectisome and its components. Left and middle panels show surface representations of 3D reconstructions of NCs based on cryo-electron microscopic data. Right panel shows a drawing of the T3S holo-complex indicating all its components. From Diepold and Wagner, 2013.

The EPEC EscF is a 8-kDa protein (Wilson *et al.*, 2001), showing homology to the major components of T3SS needle structures of Salmonella (PrgI, 24% identity), *Shigella* (MxiH, 25% identity), and *Yersinia enterocolitica* (YscF, 20% identity) (Ogino *et al.,* 2006). The EspA forms a hollow filament with helical symmetry with 5.6 subunits/turn for a 1 start helix and an inner channel permitting translocation of proteins (Daniell *et al.*, 2003). The formation of the EspA filament is dependent on T3S and EscN (the T3SS ATPase), EscC (the outer membrane secretin) and EscF. The polymerization of EspA filaments is mediated by coiled–coil interaction between subunit polypeptides (Delahay *et al*., 1999) in the same way as flagella are assembled from flagellin (Hyman and Trachtenberg, 1991).

The flagella and injectisomes have considerable organizational similarity, pointing to common and specialized functions of the different T3SS parts. Phylogenetic studies suggested that both systems share a common ancestor (Gophna *et al*., 2003). In particular, the basal structures are very similar. The needle structure of the T3SS corresponds to the flagellar hook

(Daniell, 2001). The EspA filament has approximately half the diameter of flagellum (120 vs 230 Å) and is required for effector injection as opposed to bacterial motility.

D. Control of the needle length

This regulated length of the needles has been explained in *Yersinia* by the "molecular ruler" model. In this model, the type III substrate SctP is presumed to "measure" the length of the needle by being physically stretched by the extending needle. In agreement with this model, there is a correlation between the number of the residues in a central domain of SctP and the needle filament length. Upon maximal SctP extension, a signal is transmitted leading to a stall of secretion of the needle component and recognition switch towards tip complex components (Notti and Stebbins, 2016). Alternatively, in the case of *Salmonella,* Marlovits *et al*., suggested that SctP regulates the needle length through control of the inner rod assembly. This alternate model is based on the observation that mutants lacking SctP show a decrease density in the inner rod-supporting region, generating long needles (Marlovits *et al.*, 2006). Thus, the same team proposed that SctI and SctF are simultaneously secreted and that the completion of the inner rod assembly terminates needle growth in a SctP-dependent manner. Consistent with this model, the overexpression of SctF or SctI leads to longer and shorter needles, respectively (Galan *et al.*, 2014).

E. Tip complex and translocon

Many of the properties of the tip complex and the translocon are not well understood, in particular in the case of EPEC. The outstanding questions are the following: how is the translocon inserted in the membrane? Is this associated with conformational changes in the needle and translocon components? How is the link between the needle and the translocon components regulated? How is the translocon pore formed? What regulates pore formation? We will review below studies pertinent to these questions in systems that have been better characterized.

After the assembly of the needle tip complex, the T3SS is inactive. Although it remains inactive, it does not secrete effector proteins efficiently. This “standby mode” requires the presence of a “plug” protein complex including a “gate-keeper” protein (SctW), which is thought to be located at the cytosolic interface of the injectisome; as well as the tip complex components, consisting of a hydrophilic and the major hydrophobic proteins.

Translocation of effector proteins into the eukaryotic cell cytosol requires the T3SS translocon, inserted into the host plasma membrane upon cell contact. After the host cell contact the minor hydrophobic protein of the translocon (EspB in EPEC) is secreted (Figure 5).

The translocon consists of two hydrophobic proteins, a major and minor one: in the case of EPEC, these hydrophobic proteins are EspD, the major component and EspB, the minor component (Mueller and Cornelis, 2008).

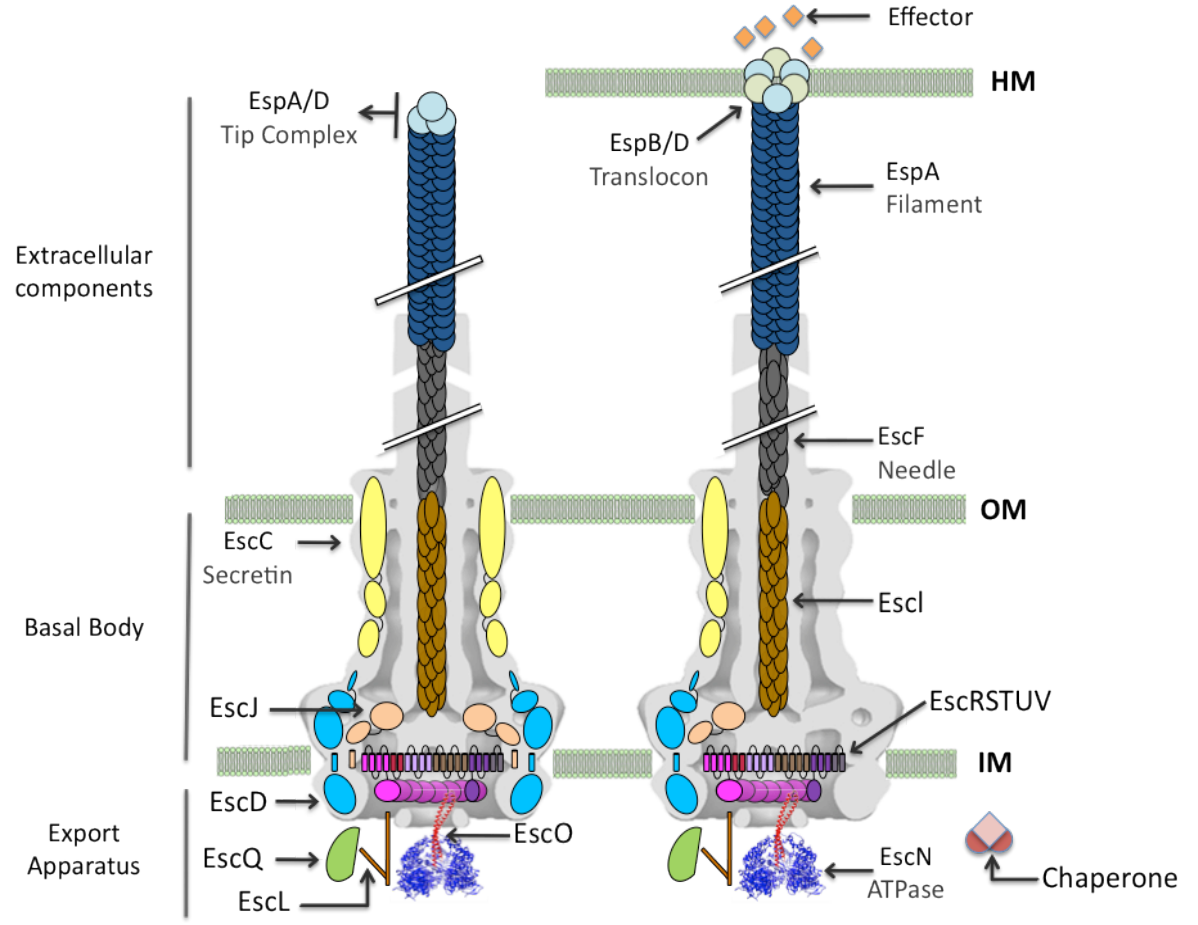

Figure 5. Scheme showing the transition from the tip complex to translocon insertion upon cell contact. Modified from a figure kindly provided by Eduardo Soto from «Departamento de Genética Molecular, Instituto de Fisiología Celular Universidad Nacional Autónoma de México».

The major and minor hydrophobic components form a hetero-oligomer inserted and forming a pore in the host cell plasma membrane.

Among the different species, the tip complex and translocon components do not share extensive homology, but are believed to perform the same function. The hydrophilic

component acts as a link between the major hydrophobic protein and the T3SS needle. The needle interacts with the hydrophilic component at least in part, through its elongate coiled-coil motif observed in all T3SS hydrophilic tip proteins described to date.

In the case of *Shigella* and *Salmonella*, some studies showed that the hydrophilic protein (IpaD/SipD respectively) possesses an amino-terminal auto-chaperoning sub-domain (Notti *et al*, 2016). This hydrophilic protein's domain may prevent the premature oligomerization of the major hydrophobic component. However, this domain has not been identified in *Yersinia* or *Pseudomonas* tip complex components, suggesting that it may not represent a general feature of T3SSs.

In *Shigella* during in vitro growth, the T3SS is inactive. The composition of the tip complex has been studied under various conditions and using bacterial mutants. Picking published the first detailed characterization of the tip complex (Picking WL *et al*. 2005). After the construction of several *ipa* mutants, different tests were performed in RBC (red blood cells) membranes. Lysis of RBCs provides a read-out of the T3SS-dependent pore formation into host cell membrane and permits to measure the pore size through osmoprotection studies. The results revealed that the pore size, presumably corresponding to the translocon inner-diameter, corresponds to 2.5 to 3 nm.

Mutation in the N-terminal (aminoacid 1 to 20) of IpaD leads to a de-regulated secretion of IpaB and IpaC. These results are in accordance with the hypothesis that the tip complex serves as a T3SA plug, preventing type III secretion at basal state. Consistently, *ipaB* and *ipaD* mutants also show constitutive type III secretion. Findings of the group of William Picking suggest that at the basal state, the tip complex is composed of a homopentamer composed of five copies of the hydrophilic component IpaD. Those findings are consistent with Muller *et al.*, who showed that the TC of *Yersinia* is also formed by a homopentamer of the ortholog LcrV (Muller *et al.*, 2005). However, the TC's composition may vary depending on the growth conditions (Picking, 2016). When *Shigella* was grown to medium supplemented with 2.5 mM deoxycholate (DOC) – a concentration that simulated the physiological range observed in the human intestine – IpaB was detected on the surface of the bacteria. Immuno-labeling of the bacterial surface indicates that IpaD can be observed without IpaB, but not the opposite. How DOC leads to IpaB recruitment to the needle is not clear allowing the speculation that it is based on conformational changes induced by DOC (Stensrud *et al*., 2008). Using molecular docking simulation on the IpaD crystal structure and fluorescence energy transfer, it was predicted that DOC binds IpaD in a cleft formed by the

central coiled-coiled and the N-terminal domain of IpaD, presumed to regulate IpaB recruitment. During their travel in the intestinal lumen, bacteria encounter bile salts, including DOC, that are present at high concentrations in the host duodenum. As a result of the interaction of IpaD with bile salts, conformational changes in IpaD stimulate the recruitment of IpaB at the needle tip (Picking *et al*., 2008).

Contrarily to what is expected based on *Shigella* results, bile salts repress Salmonella T3SS and invasiveness (Wang *et al*., 2010). In *Salmonella*, bile salts repress the transcription of T3SS genes and reduce the secretion of T3SS effector (Prouty and Gunn, 2000). NMR studies indicate that bile salts interacted with nearly the same set of SipD residues. However, the largest chemical shift perturbations occurred at a distance from the predicted bile salt binding site in IpaD. These differences may explain the opposite effects of bile salts on T3SS activity observed in *Shigella* and *Salmonella*.

There is a controversy about the *Shigella* TC's composition. Ariel Blocker and colleagues found that the TC is a heteropentamer consisting of four molecules of IpaD and one molecule of IpaB (Blocker *et al*., 2008). More recent EM studies have corroborated this model (Cheung *et al.*, 2015). In this model, the four IpaD copies are proposed to assemble first. Following secretion, the first copy of IpaD would assemble onto the needle via interaction with an MxiH subunit located below. The second, third and fourth copies of IpaD would then assemble through similar interactions with MxiH subunits as well as with a neighboring flanking IpaD copy. Because of the helical nature of the MxiH needle, the fifth site formed by the IpaD copies would differ from the others and be lined on both sites by IpaD. They assumed then that the unique nature of this site would favor the insertion of IpaB.

There are several reasons that explain the lack of precise characterization of the EPEC Tip Complex:

1) As opposed to *Shigella*, the induction of the expression of genes involved in T3SS assembly requires bacterial growth in a eukaryotic cell culture medium. Growth in this cell medium also triggers the secretion of translocator components and type III effectors in the bacterial supernatant;

2) The EPEC hydrophilic component polymerizes to form a filament, introducing another levels of complexity in the regulation. For example, the EspA filaments show different lengths and it is not clear what regulates EspA polymerization and switch to the translocon component secretion;

3) While the expression of EspA and EspD, together with that of other LEE components, is up-regulated during growth in cell medium compared to regular growth in classical bacterial culture medium, there is an additional up-regulation of EspA-D expression upon cell contact, indicative of other levels of control. For all these reasons, it has not been possible to "freeze" the system in a configuration where the tip complex caps the T3SS needle, prior to host cell contact.

VI. AB Toxin-like model

The fact that the coiled-coil domains of hydrophobic translocon components show analogy with pore forming toxins (Barta *et al*., 2012) supports the idea that both have common origins and oligomerization mechanisms. In the case of *Yersinia*, a model different from the canonical T3SS model has been proposed (Edgren *et al*., 2012). This model resembles the classical AB5 toxin delivery mechanism and is based on the following observations. Akopyan and colleagues performed immunoelectron microscopy of HeLa cells infected with *Yersinia pseudotuberculosis* to analyse the spatial localization of effectors upon host-cell interaction (Akopyan *et al*., 2010). They observed that the effector protein YopE was distributed at the bacterium-target cell interface and was not associated with distinct foci or macromolecular structures, as expected for T3SS canonical translocation. In addition, the bacterial outer membrane was in close contact with the host cell plasma membrane, in the absence of bridging structures. Under growth conditions at low Ca^{2+} concentrations leading to Yop protein expression, YopE was primarily found on the surface of the bacteria and not in the cytoplasm as predicted in the typical T3SS model (one step model). Moreover, the surface localized YopE did not colocalize with T3SAs. Both YopH and YopD were also mainly detected on the surface of *Y. pseudotuberculosis*. The next step was to investigate if the surface localized Yops were translocated to the HeLa cells being able to induce cytotoxicity. YopH is a phosphotyrosine phosphatase (PTPase) responsible for the inhibition of the immediate-early Ca^{2+} response during infection (Andersson *et al*., 1999). When YopH purified in vitro was added in the extracellular medium of cells infected by a *yopH* mutant, the same blockage of Ca^{2+} response was observed, but not in non-infected cells or cells infected with a T3SS-deficient strain. These findings suggest that the surface-localized YopH is translocated in cells in a T3SS-dependent manner.

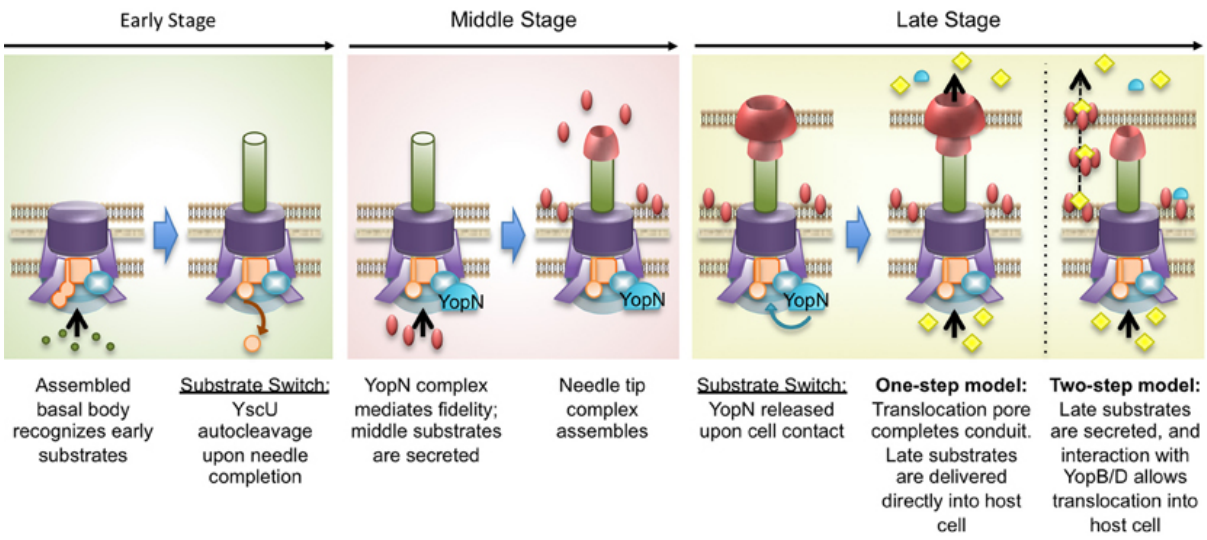

Figure 6. Progression of injectisome assembly and activation. In the early stage the assembled basal body recognizes early substrates (green) for secretion. Those substrates are required for the needle assembly. Once the needle assembly is completed, YscU (orange) undergoes autocleavage, which triggers a substrate specificity switch (middle stage). YopN associates with the basal body to allow middle substrates (red) to be secreted. Those middle substrates are required to form the tip complex and translocation pores. Upon cell contact, YopN is released from the basal body and secreted triggering the transition for the late stage. In the one-step model, the pore complex assembles at the tipoff the needle creating a continuous channel, through the late substrates (yellow) are injected. In the two-steps model, late substrates are secreted into the extracellular space and interact with pore proteins (YopB/D) allowing the translocation into the host cell. Adapted from Dewoody *et al.*, 2013.

A two-steps model is proposed whereby YopH, secreted in the extracellular medium hijacks translocon components by binding to YopB associated with host cell membranes (Akopyan *et al.,* 2011). Endocytosis of the YopB-YopH complex then accounts for YopH injection into cells. This model is reminiscent of a binary AB-toxin-like mechanism, where the major hydrophobic translocon component plays the role of the toxin B component that mediates the translocation of the catalytic A-moiety across the host-cell plasma membrane.

While this model may represent an alternate pathway for type III effector injection, these studies also raise important questions about the actual evidence for type III effectors translocation through a pore formed by the translocon in the host cell membrane.
The hydrophilic protein does not integrate the membrane, but is necessary for pore formation. Does this hydrophilic protein act as an assembly platform for proper oligomerization of the translocon components or is it mostly involved in the connection between the T3SS needle and the translocon during injection?

In the canonical view, type III effector proteins cross a sealed conduct that does not allow exchanges with the extracellular medium, to reach the host cell cytosol. In support of this view, several Cryo-EM studies show a short spacing between the bacterial surface and the host membranes at T3SS contact. In particular, a recent study showed that multiple *Chlamydia* T3SS-host membrane contact with an average spacing of 33 nm (Nans *et al*., 2015).

VII. Regulation of Pore formation by a bacterial serine protease

As described before, the T3SS-mediated injection of bacterial effector through eukaryotic cell plasma membranes requires the insertion in host cell membranes of the translocon connected to the T3SS needle by the hydrophilic protein (Fig. 7). Insertion and regulation of the translocon into the host cell membrane is a complex process. Sheahan and Isberg have identified host cell factors required for *Yersinia* T3SS-associated pore activity and showed that numerous cytoskeletal and membrane trafficking proteins are involved (Sheahan and Isberg, 2015).

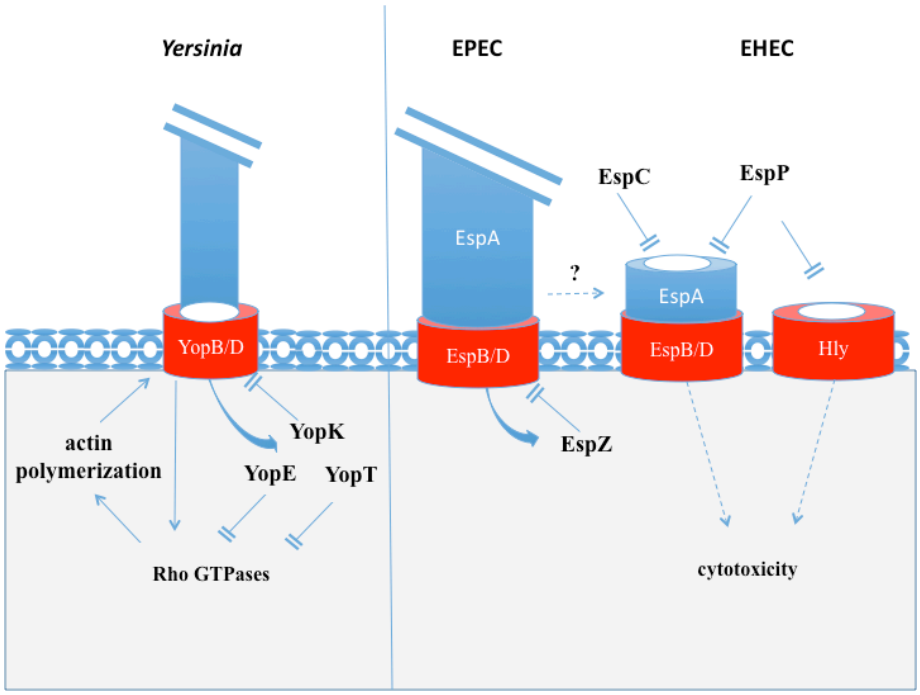

Figure 7. Bacterial effectors regulating Type3-pore formation. Adapted from Julie Guignot and Guy Tran Van Nhieu, 2016.

Briefly, upon cell contact the *Yersinia* YopB/D translocon components activate Rho GTPases leading to the polymerization of actin and T3SS-dependent pore formation (Bliska *et al*., 2013). Injected T3 effectors, such as YopK, YopE and YopT (Figure 7), downregulate T3-pore formation and effector translocation. YopK directly acts on the T3 translocon while YopE and YopT inhibit Rho GTPases (Dewoody *et al.*, 2013). In EPEC, EspZ acts in the same way as YopK, by interacting with the translocon components EspD and preventing the translocation of T3SS effector into infected cells (Berger *et al*., 2012).

Recently the host lab has reported a novel mechanism of controlling T3SS-dependent pore formation by EPEC and EHEC (Guignot *et al*., 2015). EspC is a bacterial toxin secreted by a type V (autotransporter) secretion mode. EspC belongs to the serine protease autotransporter of *Enterobacteriaceae* (SPATE) family and has been involved in EPEC virulence through its proteolytic activity on host proteins, as will be developed further. Interestingly, Guignot *et al* showed that EspC degrades the EspA and EspD components, following contact with epithelial cells, thus down-regulating T3SS-dependent pore formation and cytotoxicity. EspC does not prevent type III effector injection or actin pedestal formation, suggesting that it may recognize a specific conformation of EspA/D. It is speculated that EspC targets a complex of EspA-EspD, presumably in association with the translocon inserted in the host cell membrane. Interestingly, EspP (the EspC orthologue in EHEC) which shows the same proteolytic activity towards EspA and EspD, has been involved in the proteolytic degradation of the *E. coli* hemolysin Hly, a pore forming cytolysin, leading to the inactivation of the pore-forming activity (Brockmeyer *et al.*, 2011). These findings point to a role for these SPATEs in the controls of bacterial-induced pore in the host cell plasma membranes, and the control of host cell death and inflammatory processes.

VIII. The Serine Protease EspC

A. SPATES – General overview of EspC

SPATEs are widely spread among *Enterobacteriaceae*. SPATEs have a common structure, being composed of three different parts: a N-terminal domain composed of a cleavable peptide signal, a central passenger domain that corresponds to the mature protein with a conserved serine protease motif (GDSGSG) and a C-terminal autotransporter domain (Figure. 8). They cleave proteins implicated in diverse functions, such as fodrin, pepsin A and

hemoglobin (Dautin, 2010). Autotransporters are exported in the bacterial periplasm through the Sec pathway. They promote their secretion by using their autotransporter domain that forms a beta-barrel in the outer membrane, through which the passenger domain translocates. Following cleavage, the mature form the SPATE is released in the extracellular medium (Henderson *et al.*, 2004).

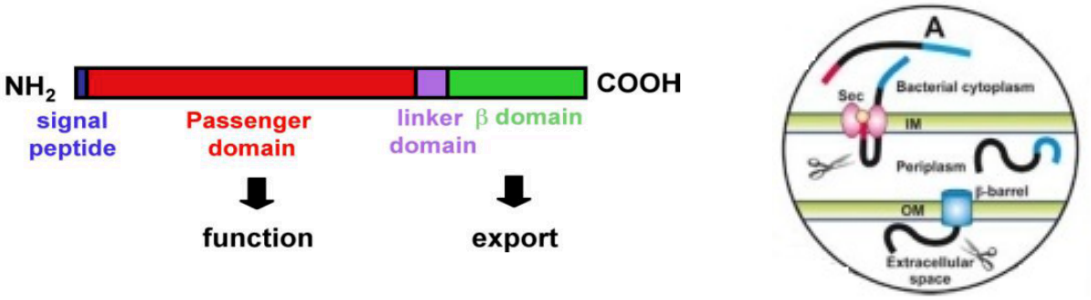

Figure 8. Autotransporter Proteins, common domain organization of AT proteins and Type V Secretion System. EspC as a SPATE is composed of 3 parts: signal peptide in the N-terminal; autotransporter (ß) domain in the C-terminal that allows the secretion of the mature protein in the extracellular milieu; passenger domain that corresponds to the mature proteins and linker domain. Adapted from (Navarro-Garcia *et al*., 2010).

EspC is the first protein secreted by EPEC during cellular infection. Even though EspC is encoded by non-LEE locus, it is regulated by Ler (Chapter V). The secretion of EspC in the extracellular milieu is independent of T3SS. However, it has been showed that while EspC secretion is T3SS-independent, EspC is translocated into the epithelial cells in a process requiring active type III secretion (Vidal and Navarro-Garcia, 2008). Indeed, EspC is detected in the cytoplasmic fraction of cells infected with wild-type EPEC, but not in an *escN* mutant deficient for the T3SS ATPase, despite the fact that the *escN* mutant secretes EspC (Vidal and Navarro-Garcia, 2008). This process is highly specific for EspC since another SPATE (Pic) is not internalized in the same conditions (Vidal and Navarro-Garcia, 2006). Interestingly, the expression of EspC is coupled to that of the T3SS suggesting a coordinated function of these virulence determinants (Guignot *et al.,* 2015). However, how exactly EspC "hijacks" the type III secretion system to gain access to the eukaryotic cell cytoplasm is not known.

B. Cytotoxicity of EspC

EspC induces the cleavage of several eukaryotic proteins, such as the coagulation factor type V, pepsin and hemoglobin (Dautin, 2010). EspC also induces the cleavage of fodrin, a protein associated with the actin cytoskeleton and two other focal adhesion proteins,

paxillin and focal adhesion kinase (FAK), following its translocation into host cells, presumably leading to cytotoxicity of epithelial cells (Navarro-Garcia *et al.,* 2004). The intracellular effects of EspC are sequential, first leading to fodrin degradation, followed by paxillin degradation, FAK dephosphorylation and FAK degradation, associated with cell rounding, cell detachment and cell death. Those events are not found in an *espC* isogenic mutant, even though this mutant causes AE lesions and is proficient for the injection of type III effectors (Navarro-Garcia *et al*., 2014).

C. EspC regulates pore formation and cytotoxicity mediated by the T3SS

Analysis of the bacterial secretion profile was the first hint of an activity of EspC on EPEC translocator components. When bacteria are grown in vitro in cell culture medium, EspC decreases the amounts of secreted EspA and EspD, while the levels of EspB are not affected (Guignot *et al*., 2015). The EspC-mediated degradation are linked to its proteolytic activity, since it is inhibited by treatment with the serine protease inhibitor PMSF, and not observed with EspC-S256I, a catalytically inactive variant. Similar effects are observed when using purified proteins. These experiments also pointed to a predominant proteolytic activity of EspC on a fraction containing EspA and EspD fraction, compared to a fraction containing EspA filaments. Immunofluorescence microscopy indicated that the EspA-EspD fraction was associated with punctiform structures, indicative of specific complexes. Consistently, EspC also regulates the levels of EspA and EspD during the early stages of cell infection by EPEC.

EspC was shown to negatively regulate the formation of T3SS-dependent pores in the plasma membrane of cells during bacterial infection, in fluorescent dye loading experiments. Increased pore formation in cells infected with the Δ*espC* mutant also increases bacterial-induced cell death, compared to WT EPEC.

RATIONALE

This Master internship builds from the hypothesis that EspC targets a specific translocon conformer that may disconnect from the T3SS needle to form a pore in the host cell membrane.

It aimed at taking advantage of the fractionation procedures worked out to isolate the EspA-EspD complex sensitive to EspC proteolysis to perform a structural characterization of this complex by electron microscopy analysis. Further, we will attempt to gain insights into the interaction between the protease and EspA-EspD by performing the structural characterization of EspC-EspA-EspD complex.

MATERIAL AND METHODS

I. Analysis of secreted proteins

All the strains used in this study are listed in the table 3.

Strains were grown in Luria-Bertani broth (LB) for 16 hours in a 37 °C shaking incubator at 200 rpm. To induce the expression of LEE genes and activate type III secretion, EPEC LB pre-cultures were diluted LB 1:200 in DMEM containing 1 g/L glucose (Gibco) and incubated for 5h at 37 °C in a 10% CO_2 incubator. The equivalent of 10 ml of bacterial culture were centrifuged at 8000 g for 10 min at 4°C.

Table 3. Bacterial strains and plasmids list.

Strain	Characteristics	Reference
WT E2348/69	EPEC wild-type strain 2348/69	(Levine et al., 1985)
Δ*espC*	*espC* isogenic mutant of WT E2348/69 (*espC*::kan)	(Guignot and Tran Van Nhieu, 2015)
Δ*espA*	*espA* isogenic mutant of WT E2348/69	(Knutton et al., 1998)
Δ*espD*	*espD* isogenic mutant of WT E2348/69	(Garmendia et al., 2004)
Δ*escN*	*escN* isogenic mutant of WT E2348/69 (*escN*::kan)	(Garmendia et al., 2004)
pJLM174	*espC* cloned in pBAD30	(Mellies et al., 2001)
pJLM174-S256I	*espC*-S256I cloned in pBAD30	(Guignot and Tran Van Nhieu, 2015)

The supernatants were filter-sterilized using a 0.22 µm-pore-size filter (Millex) and transferred to 15 ml-Falcon tubes. Proteins were subjected to precipitation using trichloroacetic acid (TCA) at a 5% final concentration for 1 hour on ice. Samples were centrifuged for 5 min at 8000 g at 4°C in a (Eppendorf, 5810 R) centrifuge. Pellets were washed with 500 µL of acetone pre-cooled at -20 °C to remove salts. Samples were immediately centrifuged for 5 min at 8000 g (Eppendorf, 5424). The wash with acetone was repeated 2 times. Pellets were resuspend in 50 µL of Laemmli loading buffer (0,0625M Tris-HCl pH 6.8; 2% SDS; 10% Glycerol; 0.005% Bromophenol Blue; 5% βME) and boiled for 10 minutes. 25 µL of each sample were analyzed by SDS-PAGE using a 12.5% polyacrylamide gel. Samples were allowed to migrate for 1h30 at a constant amperage of 25 mA and analyzed by Coomassie blue staining, by incubating for 30 min in 10% acetic acid, 50% ethanol and

40% H_2O containing 0.25% Coomassie Blue, followed by incubation successive washes in distaining buffer (6.25% acetic acid; 5% ethanol).

II. EspC Purification

To purify EspC, the strain DH5-α (pJLM174) over night (ON) LB pre-culture was diluted at 1:200 in 1 L LB medium supplemented with arabinose (0.2%) and ampicillin (100 µg/ml) at 37°C with shaking at 200 rpm for 16 h. All subsequent steps were carried at 4°C unless otherwise stated. Cultures were centrifuged at 6000 g for 15 min in a Beckman (J-26 XP) centrifuge. Clarified supernatants were filtered through a 0.22-µm-pore-size filter (Stericup, SCGPU05RE, Millipore). Proteins from filter-sterilized supernatant were precipitated by the addition of ammonium sulfate at 40% final concentration. Precipitation was performed by batch addition of the appropriate amounts of ammonium sulfate over a two hours-period, to ensure protein precipitation. Batches were added to the chilled supernatant with constant stirring, until complete crystal dissolution. Samples were centrifuged at 6000 g for 10 min. The supernatants were discarded and the pellets were resuspended in 25 mM Tris-HCl (pH 7.4), 25 mM NaCl and 1 mM β-mercaptoethanol (βME) in a volume equal to 1:50 of the supernatant. Samples were dialyzed 3 times against 100 volumes of the same buffer, using a 3.5 kD cut-off dialysis membrane (Spectra/Por, 132720). The dialyzed samples were filtered through a 0.22 µm-pore-sized filter to remove potential aggregates. Samples were subjected to FPLC (Flow Pressure Liquid Chromatography) using an anion exchange column (Mono Q, GE Healthcare) and a 20 ml 25 mM – 1000 mM NaCl linear gradient, collecting 1 ml fraction. The fractions were analyzed by SDS-PAGE and Coomassie staining, as described in *Analysis of Protein Samples* section.

III. EspA/D Purification

EspA and EspD were purified from the supernatant of Δ*espC* strain using modifications from published procedures (Guignot *et al*., 2015). The optimal growth conditions were determined in a set of pilot experiments (see Results section, (III)). Bacterial pre-cultures performed in LB were used to inoculate (dilution 1:20) DMEM cultures containing 0.1M HEPES at 37°C with 200 rpm shaking for 5 or 6 hours in a 5 liters-Erlenmeyer flask for 1 liter culture. All subsequent steps were carried at 4°C unless otherwise stated. Samples were centrifuged at 6000 g for 15 min to remove the bacteria in a Beckman (J-26 XP) centrifuge. Supernatants were filtered through 0.22-µm-pore-size filters. Proteins from the sterilized supernatant were precipitated using 40% ammonium sulfate, with constant stirring at 4°C as

described for the EspC purification protocol. Samples were centrifuged at 6000 g for 10 min at 4°C. The supernatants were discarded and pellets were resuspend in 50 mM Tris-HCl (pH 7.4), 50 mM NaCl and 1 mM β-mercaptoethanol (βME) in a volume equal to 1:50 of the supernatant. Samples were dialyzed 3 times for 1 hour against 100 volumes of the same buffer using a 3,5 kD-cut off dialysis membrane. The supernatants were filtered through 0.22-µm-pore-size filters and proteins where separated by FPLC using an anion exchange column (Mono Q, GE Healthcare) using a 20 ml-linear gradient of 50mM – 600mM NaCl, collecting 1 ml fraction. The fractions were analyzed by SDS-PAGE and Coomassie staining, as described in *Analysis of Protein Samples* section.

The fractions containing EspA and EspD, were pooled and dialyzed against 20 mM HEPES and 20 mM NaCl. The GraFix protocol was applied to the pooled fractions (Stark, 2010). The buffers were prepared based on the table 4 and filtered through a 0.22-µm-pore-size filter (Stericup, SCGPU05RE, Millipore). Using a specialized gradient mixer to form a continuous gradient a 4.4-ml centrifuge tube was filled with 2.1 ml of each buffer. 200 µl of the samples was load in the top of the gradient. The ultracentrifugation was performed at 50,000 RPM for 16h (Beckmann SW55-Ti rotor). The fractionation was performed using a capillary to pump the gradient out from the bottom to the top, taking fractions of 200 µl. The fractions were analyzed by SDS-PAGE (5% polyacrylamide gel) and Coomassie staining, as described in *Analysis of Protein Samples* section.

Table 4. Buffers composition to the gradient of GraFix procedure.

Buffer A (top)	**Buf (bottom)**
50 mM HEPES pH: 7.5	50 mM HEPES pH: 7.5
50 mM NaCl	50 mM NaCl
10% Glycerol	30% Glycerol
-	0.15% Glutaraldehyde

200 µl of the pooled fraction from anion exchange column (Mono Q) were subjected to size exclusion chromatography (Superdex 200, 25 ml column, GE Healthcare) using the same buffer as the dialysis buffer, collecting 0.5 ml-fractions. Absorption ($A_{280\ nm}$) peaks were analyzed by SDS-PAGE and transmission electron microscopy following negative staining.

IV. Electron Microscopy

EspA and EspD containing samples were analyzed by transmission electron microscopy following negative staining. Before the staining of the samples, grids were placed in paper in a carbon coated machine, until the vacuum reaches a level of 10^{-5} Torr. 4 µl of each sample were applied for one minute to the glow discharged carbon coated grids (CF400, EM, USA). Samples are processed for contrasting with 2% Uranyl acetate in water. The images were recorded on Tecnai Spirit (FEI, USA) under 120kv with an Eagle (FEI, USA) 4k x 4k camera using the TIA software. The observations were done using TEM Bright Field SA 49000X.

RESULTS

I. Testing the secretion of proteins of interest

EPEC wild-type strains have distinct genotypes and express different virulence determinants, including pili and adhesins, with polymorphic alleles (Beutin *et al*., 1990; Donnenberg and Whittam, 2001). All strains express the EPEC T3SS and the translocator components EspA, EspB ad EspD. The expression levels of these proteins, however, may vary among strains, and within the same strain as a function of the culture conditions. The most studied EPEC strain is E2348/69 isolated by Levine *et al*., 1985, also used as a model in the host laboratory. We first conducted a set of pilot experiments to determine if the bacterial strains stocks produced and secreted the proteins of interest.

To this aim, strains from -80°C glycerol stocks were streaked on LB-agar plates containing the appropriate selective antibiotic (Table 1; Materials and Methods), and isolated colonies were used to inoculate bacterial LB pre-cultures. Bacterial LB cultures inoculated from the cultures were grown overnight. Bacteria were removed by centrifugation and proteins in the supernatants were subjected to precipitation using trichloroacetic acid (Materials and Methods). Samples were analyzed by SDS-PAGE and Coomassie staining.

As previously reported, under the conditions used, T3SS translocator components were the main protein species detected in the supernatants from EPEC strains (Fig. 9). These consisted of the hydrophobic translocon components EspB and EspD, migrating as a 33 and 39 kDa species, respectively, and the small hydrophilic 20 kDa EspA protein (Fig. 9). The serine protease auto-transporter EspC (110 kDa) was also detected as a major secreted proteins (Fig. 9). As expected, EspA and EspC were missing in samples from the respective mutant strains (Fig. 9). There was a problem for the *ΔespD* mutant strain, which did not present any detectable secreted proteins. Since this strain was introduced as an additional control not used for protein purification, we did not investigate this problem further.
DH5-α/pEspC and DH5-α//pEspC-S256I strains were grown in the presence of arabinose to allow expression of *espC* under the control of the P_{BAD} promoter (Mellies *et al*., 2001).

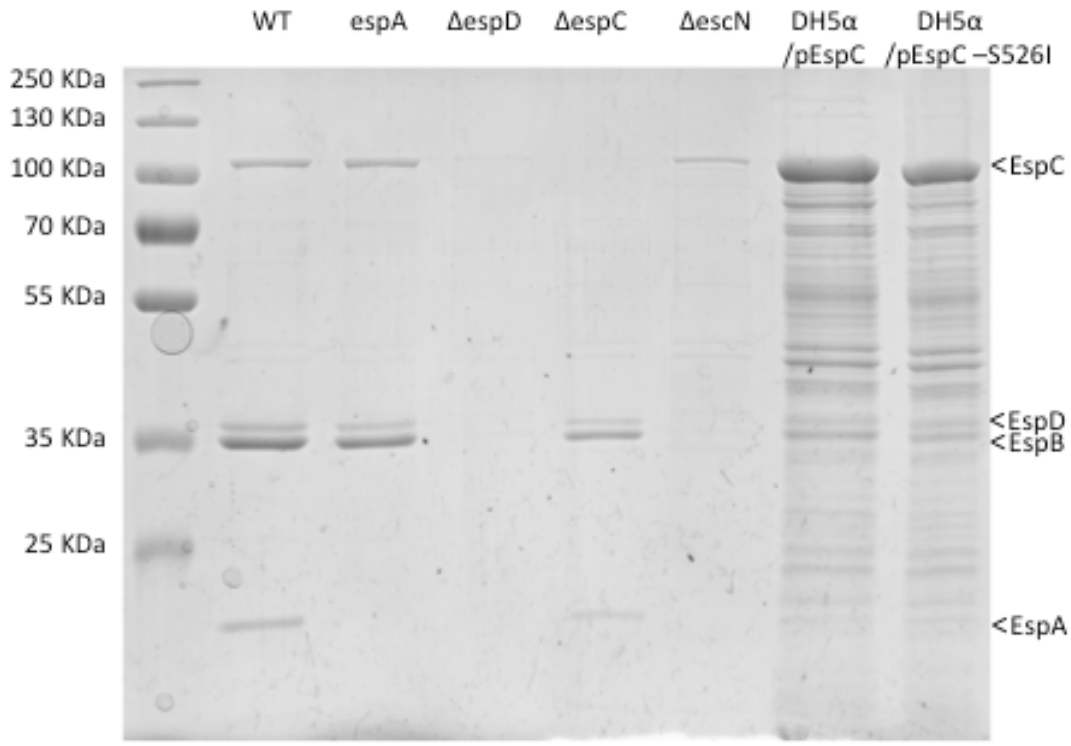

Figure 9. SDS-PAGE and Coomassie staining of proteins secreted by EPEC strains. WT E2348/69; *ΔespA*, *ΔespD*, *ΔespC* and *ΔescN* isogenic mutants. DH5-α expressing EspC (pEspC) or catalytically inactive EspC (pEspCS256I). The equivalent of 10 ml of culture supernatants of bacteria were analyzed.

As expected, the *ΔescN* mutant, deficient for the ATPase required for type III secretion, secreted EspC but not EspA, EspB or EspD (Fig. 9).

DH5-α/pEspC and DH5-α//pEspC-S256I strains showed a major band corresponding to EspC or the catalytically inactive EspC-S256I, that was not present in the supernatant of the control DH5-a parental strain (not shown). Other minor bands were also detected in the supernatants of these strains that probably corresponded to degradation products of EspC or EspC-S256I.

Together, these experiments indicate that the strains expressed and secreted the proteins of interest in amounts sufficient to proceed for their purification.

II. EspC Purification

EspC is a non-LEE-encoded serine protease autotransporter of *Enterobacteriaceae* (SPATE). It is a 110 kDa protein secreted by EPEC by a type V secretion system independently of the T3SS although EspC is translocated into the epithelial cells in a process requiring active type III secretion (Navarro-Garcia *et al*., 2008). EspC has been showed to induce cytotoxicity in host cells by interfering with the cell cytoskeleton, through the cleavage of fodrin and focal adhesions such as paxillin and Focal Adhesions Kinase (FAK) (Navarro-Garcia *et al*., 2004). However, the host lab has shown that EspC also has a role in controlling pore formation and cytotoxicity mediated by the T3SS during the early stages of infection. EspC was shown to preferentially target an EspA-EspD complex involved in T3SS-dependent pore formation, supposedly following detachment of the translocon from the T3SS needle filament. (Guignot *et al.*, 2015).

To study the interaction between the EspC and the EspA-EspD complex, we first proceeded to the purification of mature EspC. To this aim, EspC was purified from the supernatant of the strain DH5-α / pJLM174 that expresses the entire *espC* coding region. Briefly, bacteria were grown for 16 hours (Table 1; Materials and Methods). The supernatant was concentrated by ammonium sulfate precipitation and dialysis in the chromatography buffer. Samples were subjected to Flow Pressure Liquid Chromatography using a Mono Q anion exchange column and a linear NaCl gradient. Eluted fractions were analyzed by SDS-PAGE and Coomassie Blue staining.

The mature full length EspC passenger domain, migrating with an apparent molecular weight of 110 kDa, eluted as previously reported, at 265 mM NaCl (Figure 10a, fractions 4 and 5). The mature form of catalytically inactive EspC-S256I also eluted in at 265 mM NaCl (Fig. 10b, fractions 5 and 6), but also between 400 and 500 mM NaCl (Fig. 10b, fractions 10-12). In all cases, several faster migrating bands were observed probably corresponding to degradation products due to the absence of protease inhibitor during the purification steps.

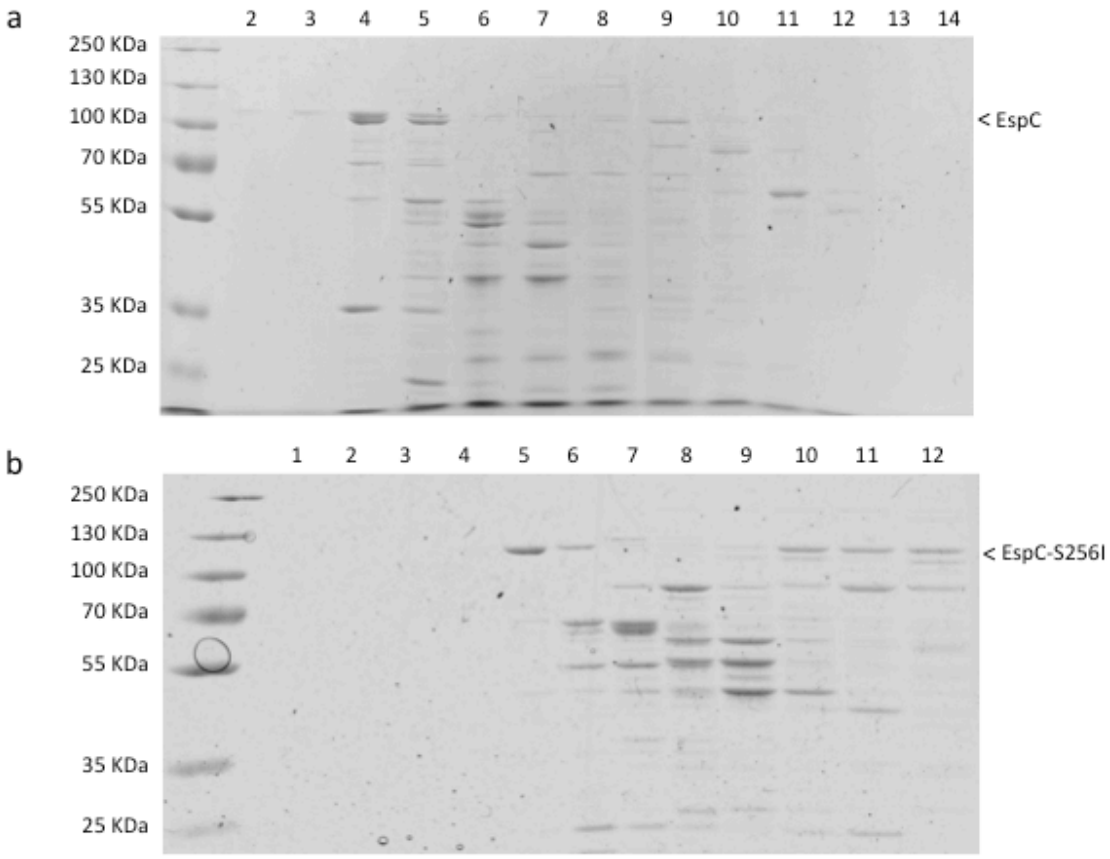

Figure 10. SDS-PAGE and Coomassie Blue analysis of de fractions from anion-exchange chromatography (MonoQ) . Full length EspC or EspC-256I are indicated with arrowheads.

III. EspA-EspD Purification

Genes encoding EspA, EspD and also EspB are organized in the same LEE operons. The synthesis and secretion of those proteins are up-regulated when bacteria grow at 37ºC in tissue culture medium in the presence of micronutrients and signals produced by eukaryotic cells. EspA and EspD are presumed to form the tip complex of EPEC. In *Shigella*, it has been proposed that the tip complex is either a homo-pentamer of IpaD or a heteropentamer composed of four copies of IpaD and one of IpaB (Pikings *et al*., 2005; Cheung *et al*., 2015). In EPEC, the tip complex has not been visualized or characterized.

The levels of expression and secretion of EPEC T3SS substrates depend on culture conditions (Kenny *et al*., in 1997). To determine the optimal conditions for the production of secreted EspA and EspD, several tests were performed with different culture conditions.

A. Testing the levels of protein production

EspC is a protease that targets specifically EspA-EspD. In order to have those complexes purified the experiments were performed using the *ΔespC* strain.

In preliminary experiments using in vitro grown bacteria, we found that EspA and EspD were present in bacterial supernatants at inconsistent levels. Previous published studies have reported the effects of various growth conditions on the expression and secretion levels of these proteins (Kenny *et al*., 1997). Based on these studies, we tried to increase the yield of secreted EspA and EspD by varying the concentration of $Fe(NO_3)_3$, or HEPES, changing the dilutions and the medium (LB/DMEM) of the pre-culture.

To this aim, the *ΔespC* strain was used to inoculate bacterial LB or DMEM pre-cultures. These pre-cultures were then used to inoculate cultures with different size inoculums, with presence or absence of $Fe(NO_3)_3$, and testing the effects of pH equilibration with HEPES or by incubation at 10 % CO2 (Table 5).

Table 5. Composition of the culture to test the yield of production of EspA, EspB and EspD

Sample	Pre-culture	Culture	Dilution	HEPES	37° Shake	37° 10% CO2	Fe(NO3)3
1	LB	DMEM	1:200	-	-	√	-
2	LB	DMEM	1:20	-	-	√	-
3	LB	DMEM	1:200	0.1M	√	-	-
4	LB	DMEM	1:20	0.1M	√	-	-
5	DMEM	DMEM	1:200	-	-	√	-
6	DMEM	DMEM	1:20	-	-	√	-
7	DMEM	DMEM	1:200	0.1M	√	-	-
8	DMEM	DMEM	1:20	0.1M	√	-	-
9	LB	DMEM	1:200	-	-	√	0.25 mM
10	LB	DMEM	1:200	-	-	√	-

Bacterial were grown for 5 hours at 37°C Samples were centrifuged to remove bacteria and supernatants were subjected to precipitation using trichloroacetic acid and analyzed by SDS-PAGE and Coomassie staining.

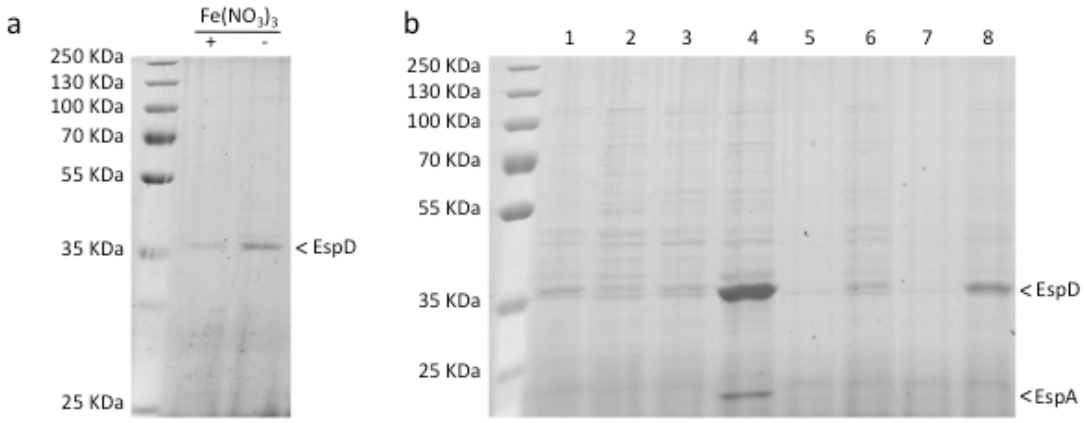

Figure 11. SDS-PAGE and Coomassie blue staining analysis proteins secreted by EPEC Δ*espC* mutant. Analysis on 12.5% polyacrylamide gel. Bacteria were grown in DMEM medium: **a**) in the presence or absence of $Fe(NO_3)_3$; **b**) in a 10 % CO_2 incubator (lanes 1, 2, 5, 6); equilibrated with 0.1M HEPES (lanes 3, 4, 7, 8); inoculated from LB pre-culture (lanes 1-4) or DMEM pre-culture (lanes 5- 8) at a 1:200 dilution (1, 3, 5, 7) or 1:20 dilution (2, 4, 6, 8).

In contrast to what was observed by Kenny *et al*., the yield of secreted EspA and EspD was not increased in medium enriched in $Fe(NO_3)_3$ (Fig. 11a). As shown in Figure 11b, as opposed to all other tested conditions, a clear increase in the yield of EspA and EspD was observed when bacteria were grown from the pre-culture in LB at a dilution of 1:20 in DMEM containing 0.1M HEPES pH 7.3. These conditions were used in all further purification of EspA and EspD experiments.

B. EspA/D Purification

The EspA/D complex purification was first performed as previously described, using anion exchange chromatography (Guignot *et al*., 2015). In pilot experiments, 200 ml of bacterial culture were analyzed (MonoQ). After several attempts to increase the yield of EspA and EspD proteins the 1 L of bacterial culture was used, growing for 6h in the conditions described above. The time of bacterial grown *in vitro* is a critical step of the study. After 4 hours of incubation, EspD is barely detected (data not shown). We thus tested bacterial cultures grown from 4 to 6 hours (Figure 14 A and B). After 5h it is possible to identify EspD in a SDS-PAGE Gel. A culture of 6 hours gives more consistent results with the stoichiometry of EspA:EspD that is the most interesting to this study.

At the initial step of the purification procedure, bacteria are removed by centrifugation. Further results shown that this is an important step. The centrifugation at 6000 g for 15 min led to substantial decrease in the amounts of EspA in subsequent steps. These

findings were not fully unexpected since EspA is known to form filaments, which may, depending on their polymerization step, pellet with bacteria at high speed spin. To avoid the loss of EspA at this initial step, removal of bacteria from cultures were performed by centrifugation at 4000 g followed by filtration through a 0.22-µm-pore-size filter. When possible, the culture was only filtered through a 0.22-µm-pore-size filter.

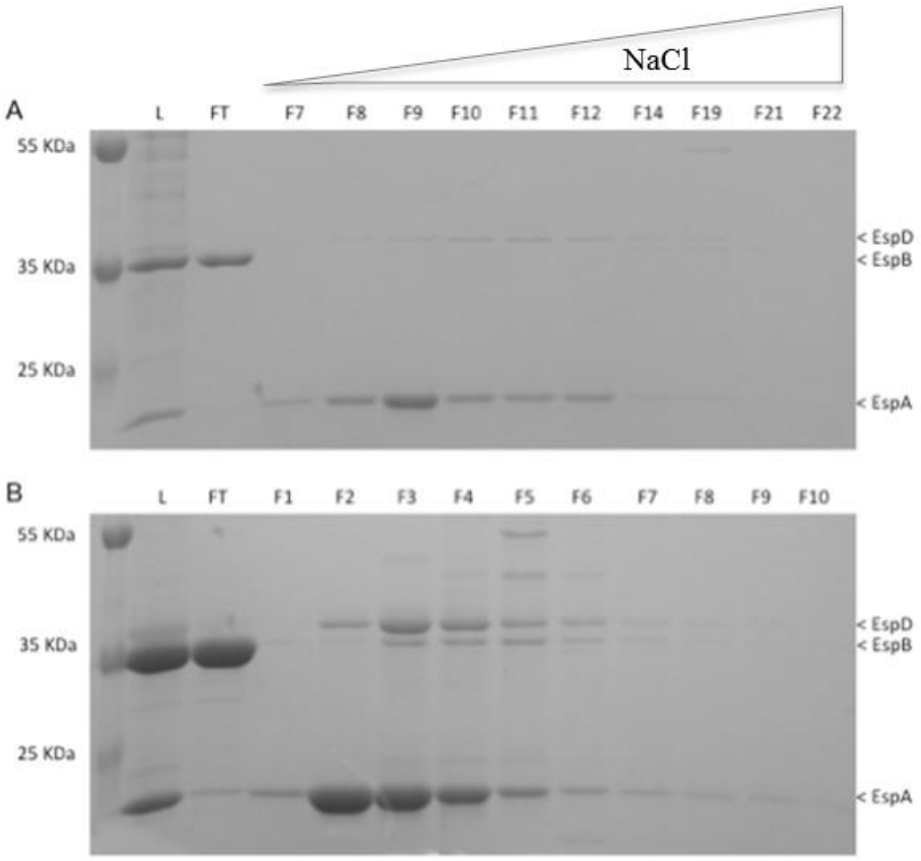

Figure 12. Analysis of proteins secreted by the Δ*espC* mutant collected from anion-exchange chromatography in each sample with interest; SDS-Page 12.5% gel with Coomassie Blue staining. Pre-culture LB diluted 1:20 in 1 L DMEM equilibrated with 0.1M HEPES. A. Culture of 5h; B. Culture of 6h.

Figure 12 shows the elution profiles of the anion exchange chromatography from samples using the previously published procedure (Fig. 12A) and the modified protocol leading to higher yield of EspA, EspB and EspD (Fig 12B). In both figures (Fig. 12), the presence of EspB, EspA and EspD was detected in the Load fraction (L). As expected EspB eluted mostly in the Flow through (FT).

As previously described, using the published procedure, EspB was mostly recovered in the flow-through, and EspA and EspD were found to co-elute at 174 mM NaCl and EspA alone eluted at 290 mM NaCl. With the new protocol, however, the previously described fractions containing only EspA eluting at higher salt concentrations were inconsistently recovered or not observed (Fig. 12A). Also, the EspD levels were also inconsistent and often low (Fig. 12A). These differences could be explained if the 5h culture time point is a critical incubation period for the expression of EspD.

A drastic increase in the yield of EspA was observed in the eluted fractions, using the modified procedure (compare Figs. 12A and 12B). For both procedures, the elution peak of EspD trailed that of EspA. Interestingly, with the new procedure, we observed an additional fraction of EspB. In addition to EspB recovered in the FT, a fraction of EspB was found to co-elute with EspD (Figure 12B).

With the recent advance in instrumentation, single particle electron microscopy (EM) and 3-D reconstruction has become a gold standard to resolve the structure of macromolecular complexes, reaching near-atomic resolution. 3D reconstruction of biological objects can be performed using methodologies with different data collection and computational strategies (Frankel *et al*., 2002). Following one methodology, an individual object, is reconstructed from multiple projections obtained by picking up pictures of the object in different positions in the EM. An object that exists in multiple copies of identical structure is reconstructed from a large number ($\sim 10^3 - 10^6$) of projections (Frank, 2010). Thus, it is important to purify particles to homogeneity. Negative staining is a method in which protein samples are embedded in a thin layer of dried heavy metal to increase the specimen contrast (Booth *et al*., 2011). EM has been used in other models as *Shigella* and *Salmonella* to visualize parts of the type III secretion system.

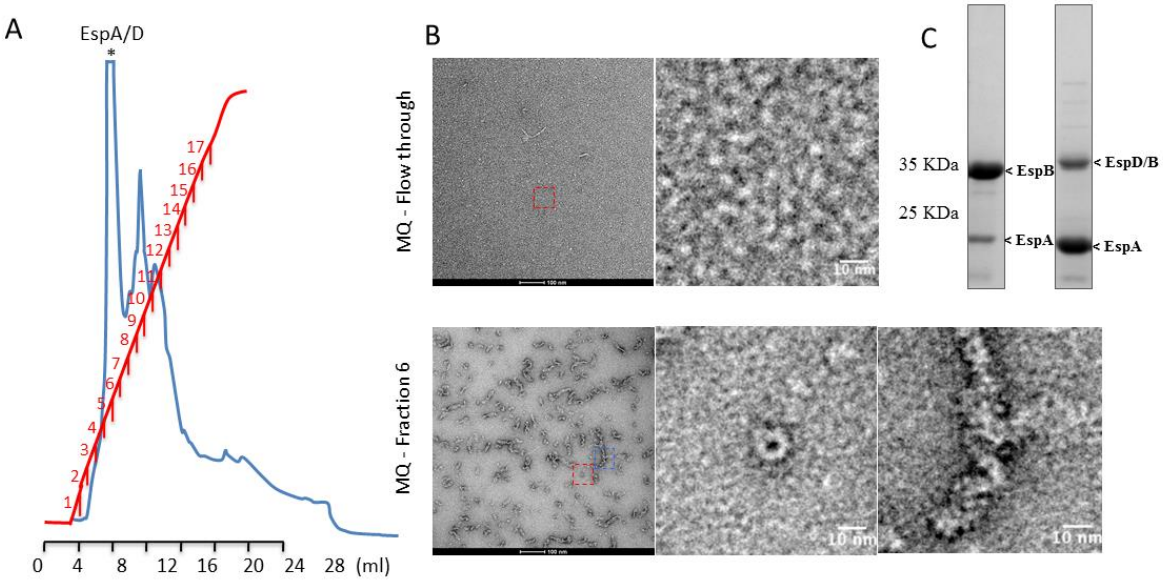

Figure 13. FPLC profile from Anion-Exchange Chromatography – MonoQ **(A)** in red the fraction number that we collected (1 ml each); in blue the OD_{280} profile using a range of 0.1 obtaining a maximum OD_{280} of 2.00. In **(B)** Electron Microscopy analysis of fractions eluted from the anion exchange chromatography. Samples were negatively stained and analyzed by transmission electron microscopy (Materials and Methods). Up: EspB (MonoQ); Down: fraction 6 from anion-exchange chromatography (MonoQ) with red zoom in the ring-like structure – EspA/D complex and blue zoom in the filamentous structures (EspA alone). (**C**) SDS-PAGE Profile of FT and 6th fractions.

We performed electron microscopy analysis of negatively stained samples to visualize EspA -D structures in samples eluted from the anion exchange chromatography.

As shown in Fig. 13B, the MonoQ flow through fraction containing EspB protein did not show any obvious defined structure, suggesting that under the conditions used, EspB did not form large oligomeric structures. Fraction 6 from the MonoQ containing EspA and EspD, however, revealed a mixture of structures: ring-like structures (Fig. 13B down), as well as filamentous structures (Fig. 13B, arrows). The ring-like structures were homogenous, with an external diameter of 10 nm and a 4 to 6 nm-inner diameter. Filamentous structures resembled EspA filaments (Figure 13B, arrows), previously observed in fractions containing only EspA (Guignot *et al*., unpublished).

To increase the purification of the fraction containing the EspA-EspD to isolate homogenous structures, we used a procedure called "GraFix" (Material and Methods; Stark, 2010.). The GraFix method combines purification by zonal ultracentrifugation with cross-linking through increasing exposure to a cross-linking reagent. This is a procedure developed to isolate large macromolecular complexes, which has been used to study structures of

secretion apparatus by EM. Unfortunately, in our case, the GraFix procedure did not allow to further fractionate the materials from the Mono Q anion exchange chromatography, since protein elution occurred as a single peak in the glycerol sedimentation gradients (data not shown). Furthermore, the procedure led to a further dilution of the materials that prevented their detection (data not shown). For these reasons, we decided not to use this procedure for subsequent purification steps of EspA and EspD.

Published reports on structures of translocon components in other systems indicate that single hydrophobic components form hexa-or heptamers (Cheung *et al*., 2015). Thus, a EspB-EspD translocon complex is predicted to have a size ranging from 200-to 300 kDa. To our knowledge, no studies have reported a complex of translocator components containing the translocon components EspB and EspD, as well as the hydrophilic component EspA. There is therefore the possibility that the EspC complex that we aim to isolate is significantly larger. Even if one assumes that EspA forms a complex with EspB-D under an oligomeric form, there are reasonable chances that such a complex would still be within the fractionation range of size exclusion chromatography (SEC).

We therefore submitted the fraction 6 eluted from the monoQ chromatography to SEC analysis, using a Superdex 200 column that enables the separation of samples with molecular mass ranging from 20 to 600 kDa. This range estimation is approximate, since gel filtration separates molecules as a function of size and shape. Hydrophobicity can also affect the migration of molecules within the SEC column matrix.

The figure 14 show the profile obtained from Superdex 200 column. While EspA could be detected in fraction 16-18, we were not able to see the presence of EspD (Fig. 14B), possibly, because of the sample dilution during the SEC procedure. Unexpectedly, a 55 kDa doublet was detected in fraction 10. The size of this double did not match the size of EspD or EspB, which were the only two other species present in the mono Q fraction analyzed by SEC. This doublet may correspond to a SDS-resistant form of an oligomer or hetero-oligomer of EspB and EspD. Unfortunately, attempts to verify the presence of EspB or EspD by Western blot analysis proved unsuccessful due to technical problems.

.

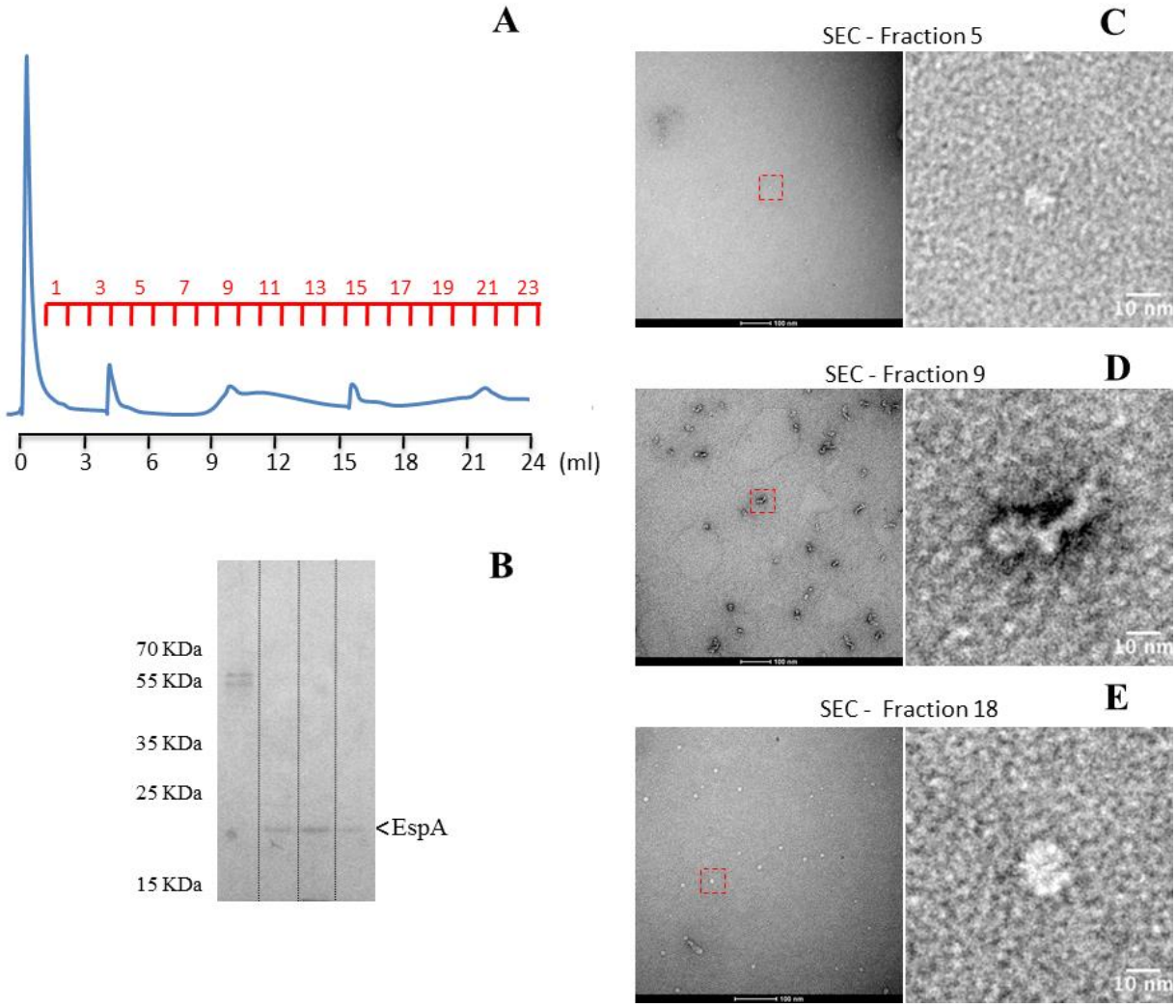

Figure 14. (A) Size Exclusion Chromatography Profile – Superdex200; in red the fraction number that we collected (1 ml each); in blue the OD_{280} profile using a range of 0.1. Visualization of Fraction 5 **(B),** fraction 9 **(C)** and fraction 18 **(D)** obtained from size exclusion chromatography.

Interestingly in the EM visualization (fig. 14) we were able to detect the presence of structures in the fractions 5, 9 and 18. In the fraction 5, homogenous and round structures were observed, with a diameter of approximately 5 nm. The fraction 9 showed a mixture of small aggregates and what appears as EspA filaments. Fraction 18 showed round structures with a diameter of 10 nm with a level of purity satisfactory for 3D-particle reconstruction.

DISCUSSION

The T3SS can be viewed as a molecular syringe that upon cell contact allows the delivery of effectors from the bacterial cytoplasm to the host cell. T3SS-dependent pore formation only happens upon bacterial cell contact, when two hydrophobic proteins forming the translocon insert into host cell plasma membrane. Although the hydrophilic protein does not insert in the membrane it is absolutely required for pore formation (Cornelis, 2006).
This project follows the hypothesis that during bacterial infection EspC targets T3SS translocon inserted into the host cell membranes that are disconnected from the T3SS needle and that would otherwise induce cytotoxicity based on their ability to form pores in the cell membrane.

The SPATE EspC is a protease able to cleave several eukaryotic proteins. It has been shown by the team of Navarro-Garcia that following its translocation into host cells, EspC leads to cytotoxicity of epithelial cells through the cleavage of Fodrin and focal adhesion proteins (Navarro-Garcia *et al.*, 2004). More recently, the host laboratory has shown that EspC also has a proteolytic activity that preferentially targets EspA and EspD. It has been shown that in vitro, as well as during cell infection, EspC leads to a decrease in the levels of secreted EspA and EspD, while the levels of secreted EspB are not affected. Further, the experiments showed a predominant proteolytic activity of EspC on fractions containing EspA and EspD compared to fractions containing EspA filaments. Consistent with the role of EspC in the negative regulation of T3SS-dependent pores in the plasma membrane of cells during bacterial infection, a Δ*espC* mutant shows increased cytotoxicity compared to WT EPEC.

These paradoxical effects of EspC on cytotoxicity could be explained by the different stages of infection. The down-regulation of pore formation by EspC presumably acts during the early stages of infection, while, at later stages EspC plays cytotoxic role by cleaving fodrin and focal adhesion proteins, following its translocation into host cells. The mechanism underlying EspC translocation into host cells is not clear. While EspC is not a T3SS substrate, it has been shown to be dependent on the T3SS. Furthermore, EspC was shown to interact with EspA in independent studies, further stressing the links between this SPATE and the T3SS. We believe that our findings that EspC targets the EPEC translocator components could provide a possible explanation for its T3SS-dependent translocation into host cells.

Indeed, the alternative to the canonical T3SS injection model in *Yersinia* (Edgren *et al.*, 2012), proposes that the major hydrophobic component acts as a B-component of the AB5-like toxin system, interacting with the host cell membrane and promoting the delivery of the bound type III effectors into host cells by an endocytic process. Since, EspC specifically targets EspA and EspD, the major translocon hydrophobic component associated with the hydrophilic component, inserted into the host cell membranes, an AB5-like mechanism may also apply to allow the translocation of EspC into host cells.

Our results have shown that the duration of bacterial growth represent a key aspect of the production of EspA and specifically EspD. An incubation window between 5 hours and 6 hours is enough to increase the yield of secreted EspD by five-fold. A possible explanation to this may be linked to the sequence of events during T3SS assembly and secretion. One possibility is that the secretion of EspA is critically timed by the molecular rulers. In this theory, when the T3SS needle reaches a determinate length, a switch determined by the molecular ruler SctP, leads to the secretion of EspA and EspD. Following 5 hours incubation and perhaps at a define EspA filament length monitored by an undefined molecular ruler, EspD would be secreted. The 6h incubation may correspond to the further processing of T3SS secretion steps leading to the release of the tip complex in the bacterial supernatant. However the point where the TC ends and the translocon begin is not entirely clear (Picking *et al*., 2016).

The steps involved in the sensing of host cells by the TC and leading to the translocation insertion into host cell membranes are not well understood. In *Shigella*, the use of point mutations in the T3SS needle component has led authors to propose a pre-translocon containing IpaB and IpaC at the needle tip prior to host cell contact (Veenendaal *et al*., 2015). The conditions to which bacteria are exposed may play a role in the composition of the complex at the needle tip. Leverton showed that when EPEC was grown to mid-log phase in DMEM versus LB medium, there was an approximate five-fold increase in transcription of LEE4 encoding EspA, EscF, EspB and EspD (Leverton and Kaper, 2005). When using a culture of 6 hours (Results, Figure 12B), we are able to co-purify EspA, EspB and EspD in the same fraction. Since the bulk of EspB does not bind to the MonoQ column, this suggests that this fraction contains EspB under a different conformation or in complex with EspA-EspD leading to its interaction with the anion exchange matrix.

In recent years, electron microscopy (EM) became one of the most important tools in the field of biological research (Arnold *et al*., 2016). Based on improved instrumentation, through direct electron detection cameras and advances in image processing software system, it is now possible to achieve good results with increasingly less concentration per volume of samples. Negative stain EM is a powerful tool that can be use to study 3D structures of macromolecular complexes or large proteins (Booth *et al*., 2011). It is also extremely important to visualize protein complexes in different conformations or simply to visualize the homogeneity or heterogeneity of purified proteins samples, providing feedbacks to improve protein purification procedures.

The purification of the proteins of interest was performed using Anion Exchange Flow Pressure Liquid Chromatography. We were able to purify the complexes of EspA-EspD repeatedly obtaining the same set of images. We could observe ring-like structures (Results, figure 13) with an outer diameter around 10 nm and an inner around 4 nm. Those values correspond to the range expected from assays performed in RBCs that studied the pore size through osmoprotection studies, using different *ipa* mutants (Picking *et al.*, 2005). Although we could see the ring-like structures the goal was to increase the purification of the samples since we still had a lot of background noise, as aggregates and what seem to be filaments, presumably formed by the excess of EspA protein.

GraFix procedure is a protocol that combines purification by ultracentrifugation with cross-linking reagent (Stark, 2010). In our case this approach did not work either because we did not have the necessary concentration for this procedure either it is more appropriate for larger structures. We submitted then the samples to gel filtration using Size-Exclusion Chromatography (SEC) where, proteins are fractionated according to their size and shape. Interestingly, we could obtain fractions with homogenous spherical structures (Results, Figure 14). These structures eluted with an elution volume corresponding to very small globular proteins with an estimated size around 14 kDa. From their size estimated by EM, however, the ring-structures are expected to correspond to oligomeric structures of much higher molecular weight. Their atypical elution volume can be explained if the elution of these structures is delayed by interaction with the column matrix, as observed for example for highly hydrophobic proteins. Although we expect these oligomeric structures to contain EspD or EspB, we could not definitely prove this. Differently of what was expected, the SDS-Page Gel analyses of the fraction from the Superdex200 showed a 55 kDa doublet (Figure 14B).

We suspect that this doublet could correspond to oligomeric or hetero-oligomeric forms of EspB and EspD. Further purification combined with mass spectrometry analysis should clarify this point.

The aim of the work was to characterize the structure of EspA-EspD targeted by EspC. An extension of this work implicates the isolation and structural characterization of EspA-EspD structures in complex with proteolytically inactive EspC. The comparative analysis EspA-EspD structures obtained in the presence or absence of EspC should give structural insights into the mode of interaction between the EspC protease and EPEC translocator components. Mass spectrometry can be applied to analyze EspC that selectively targets EspA-EspD structures or fodrin. The differences in the sensibility of EspC can be compared in order to evaluate the specific role of EspC in the infection processes and the possible alternative AB5-like toxin model.

REFERENCES

Abby, S.S., and Rocha, E.P.C. (2012). The Non-Flagellar Type III Secretion System Evolved from the Bacterial Flagellum and Diversified into Host-Cell Adapted Systems. PLoS Genet *8*.

Akopyan, K., Edgren, T., Wang-Edgren, H., Rosqvist, R., Fahlgren, A., Wolf-Watz, H., and Fallman, M. (2011). Translocation of surface-localized effectors in type III secretion. Proc. Natl. Acad. Sci. U.S.A. *108*, 1639–1644.

Andersson, K., Magnusson, K.E., Majeed, M., Stendahl, O., and Fällman, M. (1999). Yersinia pseudotuberculosis-induced calcium signaling in neutrophils is blocked by the virulence effector YopH. Infect. Immun. *67*, 2567–2574.

Arnold, S.A., Albiez, S., Opara, N., Chami, M., Schmidli, C., Bieri, A., Padeste, C., Stahlberg, H., and Braun, T. (2016). Total Sample Conditioning and Preparation of Nanoliter Volumes for Electron Microscopy. ACS Nano *10*, 4981–4988.

Barta, M.L., Dickenson, N.E., Patil, M., Keightley, A., Wyckoff, G.J., Picking, W.D., Picking, W.L., and Geisbrecht, B.V. (2012). The structures of coiled-coil domains from type III secretion system translocators reveal homology to pore-forming toxins. J. Mol. Biol. *417*, 395–405.

Berger, C.N., Crepin, V.F., Baruch, K., Mousnier, A., Rosenshine, I., and Frankel, G. (2012). EspZ of enteropathogenic and enterohemorrhagic Escherichia coli regulates type III secretion system protein translocation. MBio *3*.

Beutin, L., Orskov, I., Orskov, F., Zimmermann, S., Prada, J., Gelderblom, H., Stephan, R., and Whittam, T.S. (1990). Clonal diversity and virulence factors in strains of Escherichia coli of the classic enteropathogenic serogroup O114. J. Infect. Dis. *162*, 1329–1334.

Bhatt, S., Romeo, T., and Kalman, D. (2011). Honing the message: post-transcriptional and post-translational control in attaching and effacing pathogens. Trends Microbiol. *19*, 217–224.

Bliska, J.B., Wang, X., Viboud, G.I., and Brodsky, I.E. (2013). Modulation of innate immune responses by Yersinia type III secretion system translocators and effectors. Cell. Microbiol. *15*, 1622–1631.

Blocker, A.J., Deane, J.E., Veenendaal, A.K.J., Roversi, P., Hodgkinson, J.L., Johnson, S., and Lea, S.M. (2008). What's the point of the type III secretion system needle? Proc. Natl. Acad. Sci. U.S.A. *105*, 6507–6513.

Bogdanove, A.J., Wei, Z.M., Zhao, L., and Beer, S.V. (1996). Erwinia amylovora secretes harpin via a type III pathway and contains a homolog of yopN of Yersinia spp. J. Bacteriol. *178*, 1720–1730.

Booth, D.S., Avila-Sakar, A., and Cheng, Y. (2011). Visualizing Proteins and Macromolecular Complexes by Negative Stain EM: from Grid Preparation to Image Acquisition. J Vis Exp.

Botteaux, A., Kayath, C.A., Page, A.-L., Jouihri, N., Sani, M., Boekema, E., Biskri, L., Parsot, C., and Allaoui, A. (2010). The 33 carboxyl-terminal residues of Spa40 orchestrate the multi-step

assembly process of the type III secretion needle complex in Shigella flexneri. Microbiology (Reading, Engl.) *156*, 2807–2817.

Brockmeyer, J., Aldick, T., Soltwisch, J., Zhang, W., Tarr, P.I., Weiss, A., Dreisewerd, K., Müthing, J., Bielaszewska, M., and Karch, H. (2011). Enterohaemorrhagic Escherichia coli haemolysin is cleaved and inactivated by serine protease EspPα. Environ. Microbiol. *13*, 1327–1341.

Cheung, M., Shen, D.-K., Makino, F., Kato, T., Roehrich, A.D., Martinez-Argudo, I., Walker, M.L., Murillo, I., Liu, X., Pain, M., et al. (2015). Three-dimensional electron microscopy reconstruction and cysteine-mediated crosslinking provide a model of the type III secretion system needle tip complex. Mol. Microbiol. *95*, 31–50.

Clerc, P., Ryter, A., Mounier, J., and Sansonetti, P.J. (1986). Plasmid-mediated intracellular multiplication of Shigella flexneri. Ann. Inst. Pasteur Microbiol. *137A*, 315–320.

Cornelis, G.R. (2006). The type III secretion injectisome. Nat. Rev. Microbiol. *4*, 811–825.

Cornelis, G.R. (2010). The type III secretion injectisome, a complex nanomachine for intracellular "toxin" delivery. Biol. Chem. *391*, 745–751.

Croxen, M.A., and Finlay, B.B. (2010). Molecular mechanisms of Escherichia coli pathogenicity. Nat. Rev. Microbiol. *8*, 26–38.

Croxen, M.A., Law, R.J., Scholz, R., Keeney, K.M., Wlodarska, M., and Finlay, B.B. (2013). Recent advances in understanding enteric pathogenic Escherichia coli. Clin. Microbiol. Rev. *26*, 822–880.

Daniell, S.J., Takahashi, N., Wilson, R., Friedberg, D., Rosenshine, I., Booy, F.P., Shaw, R.K., Knutton, S., Frankel, G., and Aizawa, S. (2001). The filamentous type III secretion translocon of enteropathogenic Escherichia coli. Cell. Microbiol. *3*, 865–871.

Daniell, S.J., Kocsis, E., Morris, E., Knutton, S., Booy, F.P., and Frankel, G. (2003). 3D structure of EspA filaments from enteropathogenic Escherichia coli. Mol. Microbiol. *49*, 301–308.

Dautin, N. (2010). Serine Protease Autotransporters of Enterobacteriaceae (SPATEs): Biogenesis and Function. Toxins (Basel) *2*, 1179–1206.

Dean, P., and Kenny, B. (2009). The effector repertoire of enteropathogenic E. coli: ganging up on the host cell. Curr. Opin. Microbiol. *12*, 101–109.

Delahay, R.M., Knutton, S., Shaw, R.K., Hartland, E.L., Pallen, M.J., and Frankel, G. (1999). The coiled-coil domain of EspA is essential for the assembly of the type III secretion translocon on the surface of enteropathogenic Escherichia coli. J. Biol. Chem. *274*, 35969–35974.

Dewoody, R., Merritt, P.M., and Marketon, M.M. (2013). Regulation of the Yersinia type III secretion system: traffic control. Yersinia *3*, 4.

Diepold, A., and Wagner, S. (2014). Assembly of the bacterial type III secretion machinery. FEMS Microbiol Rev *38*, 802–822.

Diepold, A., Amstutz, M., Abel, S., Sorg, I., Jenal, U., and Cornelis, G.R. (2010). Deciphering the assembly of the Yersinia type III secretion injectisome. EMBO J. *29*, 1928–1940.

Diepold, A., Wiesand, U., Amstutz, M., and Cornelis, G.R. (2012). Assembly of the Yersinia injectisome: the missing pieces. Mol. Microbiol. *85*, 878–892.

Donnenberg, M.S. (2000). Pathogenic strategies of enteric bacteria. Nature *406*, 768–774.

Donnenberg, M.S., and Finlay, B.B. (2013). Combating enteropathogenic Escherichia coli (EPEC) infections: the way forward. Trends Microbiol. *21*, 317–319.

Donnenberg, M.S., and Kaper, J.B. (1992). Enteropathogenic Escherichia coli. Infect. Immun. *60*, 3953–3961.

Donnenberg, M.S., and Whittam, T.S. (2001). Pathogenesis and evolution of virulence in enteropathogenic and enterohemorrhagic Escherichia coli. J Clin Invest *107*, 539–548.

Edgren, T., Forsberg, A., Rosqvist, R., and Wolf-Watz, H. (2012). Type III secretion in Yersinia: injectisome or not? PLoS Pathog. *8*, e1002669.

Egan, F., Barret, M., and O'Gara, F. (2014). The SPI-1-like Type III secretion system: more roles than you think. Front Plant Sci *5*, 34.

Elliott, S.J., Sperandio, V., Girón, J.A., Shin, S., Mellies, J.L., Wainwright, L., Hutcheson, S.W., McDaniel, T.K., and Kaper, J.B. (2000). The Locus of Enterocyte Effacement (LEE)-Encoded Regulator Controls Expression of Both LEE- and Non-LEE-Encoded Virulence Factors in Enteropathogenic and Enterohemorrhagic Escherichia coli. Infect Immun *68*, 6115–6126.

Enninga, J., Mounier, J., Sansonetti, P., and Tran Van Nhieu, G. (2005). Secretion of type III effectors into host cells in real time. Nat. Methods *2*, 959–965.

Frank, J. (2010). The Ribosome Comes Alive. Isr J Chem *50*, 95–98.

Frankel, G., Phillips, A.D., Rosenshine, I., Dougan, G., Kaper, J.B., and Knutton, S. (1998). Enteropathogenic and enterohaemorrhagic Escherichia coli: more subversive elements. Mol. Microbiol. *30*, 911–921.

Galán, J.E., Lara-Tejero, M., Marlovits, T.C., and Wagner, S. (2014). Bacterial type III secretion systems: specialized nanomachines for protein delivery into target cells. Annu. Rev. Microbiol. *68*, 415–438.

Gophna, U., Ron, E.Z., and Graur, D. (2003). Bacterial type III secretion systems are ancient and evolved by multiple horizontal-transfer events. Gene *312*, 151–163.

Guignot, J., and Tran Van Nhieu, G. (2016). Bacterial Control of Pores Induced by the Type III Secretion System: Mind the Gap. Front Immunol *7*.

Guignot, J., Segura, A., and Tran Van Nhieu, G. (2015). The Serine Protease EspC from Enteropathogenic Escherichia coli Regulates Pore Formation and Cytotoxicity Mediated by the Type III Secretion System. PLoS Pathog. *11*, e1005013.

Hodgkinson, J.L., Horsley, A., Stabat, D., Simon, M., Johnson, S., da Fonseca, P.C.A., Morris, E.P., Wall, J.S., Lea, S.M., and Blocker, A.J. (2009). Three-dimensional reconstruction of the Shigella T3SS transmembrane regions reveals 12-fold symmetry and novel features throughout. Nat. Struct. Mol. Biol. *16*, 477–485.

Hyman, H.C., and Trachtenberg, S. (1991). Point mutations that lock Salmonella typhimurium flagellar filaments in the straight right-handed and left-handed forms and their relation to filament superhelicity. J. Mol. Biol. *220*, 79–88.

Iguchi, A., Thomson, N.R., Ogura, Y., Saunders, D., Ooka, T., Henderson, I.R., Harris, D., Asadulghani, M., Kurokawa, K., Dean, P., et al. (2009). Complete genome sequence and comparative genome analysis of enteropathogenic Escherichia coli O127:H6 strain E2348/69. J. Bacteriol. *191*, 347–354.

Kaas, R.S., Friis, C., Ussery, D.W., and Aarestrup, F.M. (2012). Estimating variation within the genes and inferring the phylogeny of 186 sequenced diverse Escherichia coli genomes. BMC Genomics *13*, 577.

Kaper, J.B., Nataro, J.P., and Mobley, H.L. (2004). Pathogenic Escherichia coli. Nat. Rev. Microbiol. *2*, 123–140.

Kenny, B., Abe, A., Stein, M., and Finlay, B.B. (1997). Enteropathogenic Escherichia coli protein secretion is induced in response to conditions similar to those in the gastrointestinal tract. Infect. Immun. *65*, 2606–2612.

Knutton, S., Rosenshine, I., Pallen, M.J., Nisan, I., Neves, B.C., Bain, C., Wolff, C., Dougan, G., and Frankel, G. (1998). A novel EspA-associated surface organelle of enteropathogenic Escherichia coli involved in protein translocation into epithelial cells. EMBO J *17*, 2166–2176.

Kubori, T., Sukhan, A., Aizawa, S.I., and Galán, J.E. (2000). Molecular characterization and assembly of the needle complex of the Salmonella typhimurium type III protein secretion system. Proc. Natl. Acad. Sci. U.S.A. *97*, 10225–10230.

Kudryashev, M., Stenta, M., Schmelz, S., Amstutz, M., Wiesand, U., Castaño-Díez, D., Degiacomi, M.T., Münnich, S., Bleck, C.K., Kowal, J., et al. (2013). In situ structural analysis of the Yersinia enterocolitica injectisome. Elife *2*, e00792.

Leverton, L.Q., and Kaper, J.B. (2005). Temporal Expression of Enteropathogenic Escherichia coli Virulence Genes in an In Vitro Model of Infection. Infect Immun *73*, 1034–1043.

Marlovits, T.C., Kubori, T., Sukhan, A., Thomas, D.R., Galán, J.E., and Unger, V.M. (2004). Structural insights into the assembly of the type III secretion needle complex. Science *306*, 1040–1042.

Marlovits, T.C., Kubori, T., Lara-Tejero, M., Thomas, D., Unger, V.M., and Galán, J.E. (2006). Assembly of the inner rod determines needle length in the type III secretion injectisome. Nature *441*, 637–640.

Mellies, J.L., Barron, A.M.S., and Carmona, A.M. (2007). Enteropathogenic and Enterohemorrhagic Escherichia coli Virulence Gene Regulation. Infect. Immun. *75*, 4199–4210.

Michiels, T., Vanooteghem, J.C., Lambert de Rouvroit, C., China, B., Gustin, A., Boudry, P., and Cornelis, G.R. (1991). Analysis of virC, an operon involved in the secretion of Yop proteins by Yersinia enterocolitica. J. Bacteriol. *173*, 4994–5009.

Mota, L.J., Sorg, I., and Cornelis, G.R. (2005). Type III secretion: the bacteria-eukaryotic cell express. FEMS Microbiol. Lett. *252*, 1–10.

Moura, R.A., Sircili, M.P., Leomil, L., Matté, M.H., Trabulsi, L.R., Elias, W.P., Irino, K., and Pestana de Castro, A.F. (2009). Clonal relationship among atypical enteropathogenic Escherichia coli strains isolated from different animal species and humans. Appl. Environ. Microbiol. *75*, 7399–7408.

Mueller, C.A., Broz, P., Müller, S.A., Ringler, P., Erne-Brand, F., Sorg, I., Kuhn, M., Engel, A., and Cornelis, G.R. (2005). The V-antigen of Yersinia forms a distinct structure at the tip of injectisome needles. Science *310*, 674–676.

Mueller, C.A., Broz, P., and Cornelis, G.R. (2008). The type III secretion system tip complex and translocon. Mol. Microbiol. *68*, 1085–1095.

Nans, A., Kudryashev, M., Saibil, H.R., and Hayward, R.D. (2015). Structure of a bacterial type III secretion system in contact with a host membrane in situ. Nat Commun *6*, 10114.

Nataro, J.P., and Kaper, J.B. (1998). Diarrheagenic Escherichia coli. Clin. Microbiol. Rev. *11*, 142–201.

Navarro-García, F., Canizalez-Roman, A., Sui, B.Q., Nataro, J.P., and Azamar, Y. (2004). The serine protease motif of EspC from enteropathogenic Escherichia coli produces epithelial damage by a mechanism different from that of Pet toxin from enteroaggregative E. coli. Infect. Immun. *72*, 3609–3621.

Navarro-Garcia, F., Serapio-Palacios, A., Vidal, J.E., Salazar, M.I., and Tapia-Pastrana, G. (2014). EspC promotes epithelial cell detachment by enteropathogenic Escherichia coli via sequential cleavages of a cytoskeletal protein and then focal adhesion proteins. Infect. Immun. *82*, 2255–2265.

Nguyen, R.N., Taylor, L.S., Tauschek, M., and Robins-Browne, R.M. (2006). Atypical Enteropathogenic Escherichia coli Infection and Prolonged Diarrhea in Children. Emerg Infect Dis *12*, 597–603.

Notti, R.Q., and Stebbins, C.E. (2016). The Structure and Function of Type III Secretion Systems. Microbiol Spectr *4*.

Ochoa, T.J., Barletta, F., Contreras, C., and Mercado, E. (2008). New insights into the epidemiology of enteropathogenic Escherichia coli infection. Trans R Soc Trop Med Hyg *102*, 852–856.

Ogino, T., Ohno, R., Sekiya, K., Kuwae, A., Matsuzawa, T., Nonaka, T., Fukuda, H., Imajoh-Ohmi, S., and Abe, A. (2006). Assembly of the Type III Secretion Apparatus of Enteropathogenic Escherichia coli. J. Bacteriol. *188*, 2801–2811.

Parham, N.J., Srinivasan, U., Desvaux, M., Foxman, B., Marrs, C.F., and Henderson, I.R. (2004). PicU, a second serine protease autotransporter of uropathogenic Escherichia coli. FEMS Microbiol. Lett. *230*, 73–83.

Picking, W.L., and Picking, W.D. (2016). The Many Faces of IpaB. Front. Cell. Infect. Microbiol 12.

Picking, W.L., Nishioka, H., Hearn, P.D., Baxter, M.A., Harrington, A.T., Blocker, A., and Picking, W.D. (2005). IpaD of Shigella flexneri is independently required for regulation of Ipa protein secretion and efficient insertion of IpaB and IpaC into host membranes. Infect. Immun. *73*, 1432–1440.

Poyraz, O., Schmidt, H., Seidel, K., Delissen, F., Ader, C., Tenenboim, H., Goosmann, C., Laube, B., Thünemann, A.F., Zychlinsky, A., et al. (2010). Protein refolding is required for assembly of the type three secretion needle. Nat. Struct. Mol. Biol. *17*, 788–792.

Prouty, A.M., and Gunn, J.S. (2000). Salmonella enterica serovar typhimurium invasion is repressed in the presence of bile. Infect. Immun. *68*, 6763–6769.

Radics, J., Königsmaier, L., and Marlovits, T.C. (2014). Structure of a pathogenic type 3 secretion system in action. Nat. Struct. Mol. Biol. *21*, 82–87.

Rosenshine, I., Ruschkowski, S., and Finlay, B.B. (1996). Expression of attaching/effacing activity by enteropathogenic Escherichia coli depends on growth phase, temperature, and protein synthesis upon contact with epithelial cells. Infect. Immun. *64*, 966–973.

Sal-Man, N., Setiaputra, D., Scholz, R., Deng, W., Yu, A.C.Y., Strynadka, N.C.J., and Finlay, B.B. (2013). EscE and EscG are cochaperones for the type III needle protein EscF of enteropathogenic Escherichia coli. J. Bacteriol. *195*, 2481–2489.

Schraidt, O., and Marlovits, T.C. (2011). Three-dimensional model of Salmonella's needle complex at subnanometer resolution. Science *331*, 1192–1195.

Schraidt, O., Lefebre, M.D., Brunner, M.J., Schmied, W.H., Schmidt, A., Radics, J., Mechtler, K., Galán, J.E., and Marlovits, T.C. (2010). Topology and Organization of the Salmonella typhimurium Type III Secretion Needle Complex Components. PLoS Pathog *6*.

Shakhnovich, E.A., Davis, B.M., and Waldor, M.K. (2009). Hfq negatively regulates type III secretion in EHEC and several other pathogens. Mol. Microbiol. *74*, 347–363.

Shea, J.E., Hensel, M., Gleeson, C., and Holden, D.W. (1996). Identification of a virulence locus encoding a second type III secretion system in Salmonella typhimurium. Proc. Natl. Acad. Sci. U.S.A. *93*, 2593–2597.

Sheahan, K.-L., and Isberg, R.R. (2015). Identification of Mammalian Proteins That Collaborate with Type III Secretion System Function: Involvement of a Chemokine Receptor in Supporting Translocon Activity. mBio *6*.

Spears, K.J., Roe, A.J., and Gally, D.L. (2006). A comparison of enteropathogenic and enterohaemorrhagic Escherichia coli pathogenesis. FEMS Microbiol. Lett. *255*, 187–202.

Stark, H. (2010). GraFix: stabilization of fragile macromolecular complexes for single particle cryo-EM. Meth. Enzymol. *481*, 109–126.

Stensrud, K.F., Adam, P.R., La Mar, C.D., Olive, A.J., Lushington, G.H., Sudharsan, R., Shelton, N.L., Givens, R.S., Picking, W.L., and Picking, W.D. (2008). Deoxycholate interacts with IpaD of

Shigella flexneri in inducing the recruitment of IpaB to the type III secretion apparatus needle tip. J. Biol. Chem. *283*, 18646–18654.

Veenendaal, A.K.J., Hodgkinson, J.L., Schwarzer, L., Stabat, D., Zenk, S.F., and Blocker, A.J. (2007). The type III secretion system needle tip complex mediates host cell sensing and translocon insertion. Mol. Microbiol. *63*, 1719–1730.

Vidal, J.E., and Navarro-García, F. (2006). Efficient translocation of EspC into epithelial cells depends on enteropathogenic Escherichia coli and host cell contact. Infect. Immun. *74*, 2293–2303.

Vidal, J.E., and Navarro-García, F. (2008). EspC translocation into epithelial cells by enteropathogenic Escherichia coli requires a concerted participation of type V and III secretion systems. Cell. Microbiol. *10*, 1975–1986.

Wang, Y., Nordhues, B.A., Zhong, D., and De Guzman, R.N. (2010). NMR characterization of the interaction of the Salmonella type III secretion system protein SipD and bile salts. Biochemistry *49*, 4220–4226.